Interaction between induced and natural variation at *oil yellow1* delays flowering in maize

Rajdeep S. Khangura[†§‡], Bala P. Venkata[†2], Sandeep R. Marla[†1], Michael V. Mickelbart[†‡], Singha Dhungana[3], David M. Braun[3], Brian P. Dilkes[§‡], Gurmukh S. Johal[†‡]

[†]Department of Botany and Plant Pathology, Purdue University, West Lafayette, Indiana 47907

[‡]Center for Plant Biology, Purdue University, West Lafayette, Indiana 47907

[§]Department of Biochemistry, Purdue University, West Lafayette, Indiana 47907

[3]Division of Biological Sciences, Interdisciplinary Plant Group, Missouri Maize Center, University of Missouri, Columbia, Missouri 65211

Current address

[1]Department of Agronomy, Kansas State University, Manhattan, Kansas 66506

[2]Donald Danforth Plant Science Center, St. Louis, Missouri 63132

Corresponding Authors

Brian P. Dilkes, 170 S. University Street, Purdue University, West Lafayette, Indiana 47907, Phone: (765) 494 2584, Email: bdilkes@purdue.edu

Gurmukh S. Johal, 915 W. State Street, Purdue University, West Lafayette, Indiana 47907, Phone: (765) 494-4448, Email: gjohal@purdue.edu

Abstract

We previously demonstrated that maize (*Zea mays*) locus *very oil yellow1 (vey1)* encodes a putative cis-regulatory expression polymorphism at the magnesium chelatase subunit I gene (aka *oil yellow1*) that strongly modifies the chlorophyll content of the dominant *Oy1-N1989* mutants. The *vey1* allele of Mo17 inbred line reduces chlorophyll content in the mutants leading to reduced photosynthetic output. *Oy1-N1989* mutants in B73 flowered four days later than wild-type. Enhancement of *Oy1-N1989* by the Mo17 allele at the *vey1* QTL delayed flowering further, resulting in detection of a flowering time QTL in two bi-parental mapping populations crossed to *Oy1-N1989*. The near isogenic lines of B73 harboring the *vey1* allele from Mo17 delayed flowering of *Oy1-N1989* mutants by twelve days. Just as previously observed for chlorophyll content, *vey1* had no effect on flowering time in the absence of the *Oy1-N1989* allele. Loss of chlorophyll biosynthesis in *Oy1-N1989* mutants and enhancement by *vey1* reduced CO_2 assimilation. We attempted to separate the effects of photosynthesis on the induction of flowering from a possible impact of chlorophyll metabolites and retrograde signaling by manually reducing leaf area. Removal of leaves, independent of the *Oy1-N1989* mutant, delayed flowering but surprisingly reduced chlorophyll contents of emerging leaves. Thus, defoliation did not completely separate the identity of the signal(s) that regulates flowering time from changes in chlorophyll content in the foliage. These findings illustrate the necessity to explore the linkage between metabolism and the mechanisms that connect it to flowering time regulation.

KEYWORDS flowering time; photosynthesis; epistasis, setaria; sorghum

45 **Introduction**

46 As sexual reproduction is necessary for the production of seeds and fruits, the onset of flowering
47 in angiosperms has been a key focus for plant biologists working on ornamental, horticultural, and
48 other crop species (Lang 1952; Zeevaart 1962; Searle 1965). The onset of reproductive
49 development in angiosperms is affected by a change in meristem identity. The vegetative to floral
50 transition of meristems commits plant development to production of floral organs and sexual
51 reproduction. The integration of signals to correctly time this transition is key to plant fitness.
52 Unsurprisingly, endogenous and environmental cues regulate flowering time (Amasino and
53 Michaels 2010; Cho *et al.* 2017; Minow *et al.* 2018). A critical environmental cue is the duration
54 of the light period, or photoperiod. The photoperiodic responses of plants influence the vegetative
55 to floral transition and the mechanisms of this response have been a focus of intensive research for
56 over a century (Klebs, 1918). Multiple non-photoperiodic cues as well as endogenous signals,
57 sometimes called the autonomous pathway, are also critical to floral transition. Endogenous signals
58 including hormones and the carbohydrate status of the plant can also play a critical role in the
59 regulation of flowering time (Corbesier *et al.* 1998; Moghaddam and Ende 2013). But
60 environmental influences, such as light quality, alter hormone biosynthesis (Lang 1957; Evans and
61 Poethig 1995; Mutasa-Göttgens and Hedden 2009), and light intensity dramatically influences
62 photosynthesis and thereby carbohydrate status (Chen *et al.* 2004). These stimuli converge through
63 the same floral integrators (named FLOWERING LOCUS T (FT) and FLOWERING LOCUS D
64 (FD) in *Arabidopsis thaliana)* for which orthologs have been identified in many flowering plants
65 (Abe *et al.* 2005; Wigge *et al.* 2005; Corbesier *et al.* 2007; Meng *et al.* 2011; Zhang *et al.* 2016).
66 Accumulation of FT and FD gene products trigger the vegetative shoot apical meristems to acquire
67 the competency to become inflorescence meristems and produce flowers in part via the activation
68 of MADS-box transcription factors that control meristem identity through APETALA1 (Abe *et al.*

69 2005; Wigge *et al.* 2005). In Arabidopsis, FT is regulated by CONSTANS (CO) in response to
70 both circadian regulation and photoperiodic responses. CONSTANS itself is regulated by the
71 MADS-box transcription factor SUPPRESSOR OF CONSTANS1 (SOC1) (Samach *et al.* 2000).
72 Maize was domesticated from teosinte (*Zea mays* ssp. *parviglumis* or spp. *mexicana*) in
73 Central America (Doebley *et al.* 1997; Wang *et al.* 1999). Strong selection on time to flower
74 contributed to the adaptation of maize to different latitudes (Salvi *et al.* 2007; Huang *et al.* 2017;
75 Swarts *et al.* 2017). Flowering of teosinte is promoted by short-day conditions. In contrast,
76 temperate maize germplasm is relatively day-neutral and flowering is primarily under the control
77 of the autonomous pathway (Coles *et al.* 2010). Several mutant and QTL studies have identified
78 loci affecting flowering time in maize (Buckler *et al.* 2009; Coles *et al.* 2010; Steinhoff *et al.* 2012;
79 Bouchet *et al.* 2017). Some of these loci include: *indeterminate1* (*id1*; Colasanti et al. 1998); *early*
80 *phase change* (*epc*; Vega et al. 2002); the maize FLORICAULA/LEAFY orthologs *zfl1* and *zfl2*
81 (Bomblies et al. 2003); *delayed flowering1* (*dlf1*; Muszynski et al. 2006); the cis-element
82 polymorphism *vegetative transitioning1* (*vgt1*; Salvi et al. 2007) that regulates a downstream
83 APETALA2-like transcription factor *zmrap2.7*; *zea mays mads4* (*zmm4*; Danilevskaya et al. 2008);
84 *zmcct10* (Hung *et al.* 2012); *zea mays centroradiales8* (*zcn8*; Meng et al. 2011); *zea mays mads1*
85 (*zmmads1*; Alter et al. 2016); and *zea mays mads69* (Liang *et al.* 2019). Many of these encode the
86 maize orthologs of genes identified as regulators of flowering in Arabidopsis. For example, *dlf1*
87 and *zcn8* encode homologs of the Arabidopsis flowering time determinants FD and FT,
88 respectively. *id1* encodes a zinc-finger transcription factor acting upstream of both DLF1 and
89 ZCN8 (Kozaki *et al.* 2004; Muszynski *et al.* 2006; Meng *et al.* 2011). *zmm4* is an activator of
90 flowering that is part of a conserved syntenic pair of MADS box genes in the grasses, with *zmm24*
91 as the neighboring gene, and encodes one of two maize paralogs of the wheat flowering time and

92 vernalization response locus VRN1 (Danilevskaya *et al.* 2008). *zmm4* acts downstream of *dlf1* and
93 *id1* in the control of flowering time in maize. *zmmads1* is a functional homolog of the Arabidopsis
94 flowering time and circadian rhythm regulator *soc1* (Alter *et al.* 2016).

95 One important endogenous signal that contributes to flowering time is the carbohydrate
96 allocation status (Ohto *et al.* 2001; Seo *et al.* 2011; Eveland and Jackson 2012; Wahl *et al.* 2013;
97 Cho *et al.* 2018). In maize, mutants that are compromised in either sugar export from source tissues
98 or loading sucrose into the phloem flower later than their congenic wild-type siblings (Braun *et al.*
99 2006; Baker and Braun 2008; Ma *et al.* 2008; Slewinski *et al.* 2009; Slewinski and Braun 2010).
100 This is not limited to maize, as starch-deficient Arabidopsis mutants exhibit delayed flowering
101 (Corbesier *et al.* 1998). Trehalose-6-phosphate (T6P) has been implicated as a reporter of the
102 energy status and Arabidopsis mutants effected in this metabolite also exhibit altered flowering
103 time (Paul 2008; Wahl et al. 2013; Seo et al. 2011). T6P and sucrose are positively correlated, and
104 low levels of T6P results in delayed flowering in Arabidopsis (Wahl *et al.* 2013). Remarkably, the
105 carbohydrate status and transcriptional regulatory genes controlling flowering time may be directly
106 linked in maize. The *id1* flowering time mutants alter carbohydrate partitioning in leaves and
107 accumulate more sucrose and starch (Coneva et al. 2012). As a result, maize flowering time gene
108 ID1 has been proposed to act as a carbohydrate status sensor that influences flowering time
109 (Coneva, Zhu, and Colasanti 2007; Minow et al. 2018). Remarkably, the promoter of the T6P
110 biosynthetic gene TPS1 is a predicted target of the ID1 DNA-binding protein and low levels of
111 T6P were observed in *id1* mutants (Minow *et al.* 2018).

112 If sugars are critical for floral transitioning in plants, then manipulation of photosynthesis
113 should alter flowering. Magnesium chelatase (MgChl) is a hetero-oligomeric enzyme complex that
114 catalyzes the first committed step of chlorophyll biosynthesis by conversion of protoporphyrin IX

115 (PPIX) into magnesium-PPIX (Walker and Weinstein 1991; Gibson et al. 1995). We previously
116 identified a cis-acting expression polymorphism at the *oil yellow1* (*oy1)* locus (Sawers *et al.* 2006)
117 associated with a QTL called *very oil yellow1* (*vey1*) that modifies the chlorophyll content of semi-
118 dominant *Oy1-N1989* mutants (Khangura *et al.* 2019). The effect of *vey1* is only visible in the
119 presence of *Oy1-N1989,* indicating that this natural variant has a cryptic effect on the function of
120 the MgChl complex. We used controlled crosses to segregate *Oy1-N1989* and the modifier alleles
121 at *vey1* to generate populations of maize with a range of chlorophyll contents. We used this
122 variation in chlorophyll to explore the effects of chlorophyll content on net CO_2 assimilation.
123 These changes in chlorophyll accumulation resulted in changes in net CO_2 assimilation and
124 photosynthetically-fixed carbon accumulation. Remarkably, we noticed that flowering time across
125 material with differing photosynthetic rates and chlorophyll contents was dramatically different.
126 We observed that *Oy1-N1989* mutants flowered later and that the reduced chlorophyll
127 accumulation was associated with a delay in flowering time. Similar to the cryptic effects of *vey1*
128 on chlorophyll content, the modifier allele had no effect on flowering time in the absence of the
129 *Oy1-N1989* mutant allele. Chlorophyll content was consistently associated with earlier flowering
130 and partial rescue of chlorophyll accumulation in the *Oy1-N1989* mutant by the *vey1* QTL
131 accelerated flowering in the mutants but had no effect on wild-type siblings. In addition to
132 measurements of net CO_2 assimilation, the premature senescence of maize leaves induced by sugar
133 accumulation, following sink removal, was also reduced by *Oy1-N1989* and further reduced by
134 *vey1* alleles that decrease chlorophyll content and net CO2 assimilation. The effect of reduced
135 photosynthate accumulation on flowering time was not specific to *Oy1-N1989* as mechanical
136 removal of leaves, to reduce plant leaf area, also delayed flowering time. Thus, all of our results

137 are consistent with an integrative measure of carbon assimilation linking energy status and
138 flowering time in maize.

139 Materials and Methods

140 Plant materials

141 The origin of *Oy1-N1989* mutant allele has been previously described (Khangura *et al.* 2019). The
142 mutant allele is maintained in B73 background and is propagated by crossing heterozygous
143 mutants (*Oy1-N1989/oy1*) to the wild-type siblings. The introgressed stock of *Oy1-N1989* into
144 B73 was used for crossing to various mapping populations. A total of 216 intermated B73 × Mo17
145 population (IBM-RILs), and 251 synthetic 10 doubled haploid lines (Syn10-DH) were crossed as
146 ear-parents with *Oy1-N1989/oy1*:B73 pollen. The pollen of *Oy1-N1989/oy1*:B73 plants were also
147 crossed on to the ears of 35 B73-Mo17 near-isogenic lines (BM-NILs) for QTL validation. Tables
148 S1-S3 contain the full list of IBM-RILs, Syn10-DH, and BM-NILs used to develop F_1 hybrid
149 populations.

150 Field trials

151 The field experiments were conducted at the Purdue Agronomy Center for Research and Education
152 (ACRE) in West Lafayette, Indiana. Each cross was evaluated as a single plot of 12-16 plants.
153 Each plot derived from crosses with *Oy1-N1989/oy1*:B73 tester segregated for both mutant and
154 wild-type siblings in approximately 1:1 ratio. Seeds were sown with tractor-driven seed planter
155 with plot length of 3.84 meters (m) with alley length of 0.79 m, and inter-row spacing of 0.79 m.
156 Rainfall was sufficient throughout the growing season and eliminated any need of irrigation.

157 Standard crop management practices at Purdue in terms of fertilizer, pest, and weed control for
158 growing field maize were adopted.

159 Each experiment was divided into blocks. Progenies of crosses of B73 and Mo17 ears to
160 *Oy1-N1989/oy1*:B73 pollen were used as parental checks in each block. Parental checks were
161 randomized with each block. The IBM-RILs F_1 populations were evaluated as a single replication
162 in 2013. Syn10-DH F_1 populations were evaluated in 2016 with two randomized replications
163 planted in randomized complete block design (RCBD). Hybrid progenies of *Oy1-N1989/oy1*:B73
164 with BM-NILs were screened in 2016 with five replications planted in RCBD.

165 **Field phenotyping and data collection**

166 The mutant plants in each plot were identified visually as pale plants. The chlorophyll content in
167 mutant and wild-type plants was approximated using a CCM-200 plus (Opti-Sciences Inc., Hudson,
168 NH) as described in Khangura *et al.* 2019. We previously demonstrated correlation of 0.94
169 between CCM-200 plus values and chlorophyll *a*, chlorophyll *b*, and total chlorophyll contents
170 (Khangura *et al.* 2019), and therefore used CCM-200 plus values (CCM) as a proxy for chlorophyll
171 content in the materials described here. CCMI refers to measurements taken with CCM-200 plus
172 instrument from 25-30 days after sowing and CCMII refers to measurements taken 45-50 days
173 after sowing. Mutants were tagged around V5-V7 stages of development. Tagging is necessary as
174 suppression of the *Oy1-N1989* mutant phenotype by *vey1* interferes with visual classification of
175 mutant and wild-type siblings at maturity. Flowering time in each F_1 population was recorded
176 separately on the wild-type and mutant plants. The date at which roughly half of the wild-type or
177 mutant plants in a given plot were shedding pollen was recorded as the date of anthesis for a given
178 genotype in that plot. Similarly, the date at which half of the wild-type or mutant plants had
179 emerging silks was recorded as the date of silking for the respective genotype in that plot. The

180 dates of anthesis and silking for both wild-type and mutant genotypes were then subtracted from
181 the date of planting to obtain respective wild-type or mutant days to anthesis (DTA), and days to
182 silking (DTS). Further, the difference between DTA and DTS was used to derive the anthesis-
183 silking interval (ASI); ASI = DTA-DTS. Wild-type and mutant traits are denoted with a prefix WT
184 and MT, respectively. Ratio and differences of these flowering times values were also calculated
185 as MT/WT and WT-MT, respectively.

186 Induced leaf senescence assay: A total of 15 F_1 populations derived from B73-like NILs ×
187 *Oy1-N1989/oy1*:B73 cross were used for this experiment. Seven of these B73-like NILs carried an
188 introgression of *vey1* from Mo17 ($vey1^{Mo17}$), whereas the other eight NILs had the B73 genotype
189 at *vey1* ($vey1^{B73}$). These NIL populations were planted in the field with at least two replications of
190 each genotype planted in RCBD. The procedure for this experiment was adapted from Sekhon *et*
191 *al.* 2012. Briefly, for the suppressing NIL, F_1 crosses of primary and secondary ears of both wild-
192 type and mutant plants were covered with shoot bags before silk emergence. After 3-4 days of
193 tassel shedding, roughly half of the shoot bags were removed, and these ears were allowed to open
194 pollinate. Staggered rows of B73 were planted on both sides of the experimental row in the field
195 to ensure pollination of exposed ears. The day of shoot exposure was marked as 0 days after
196 anthesis (DAA). For the enhancing B73 NILs, a late set of suppressed NIL F_1 was used as a control.
197 A similar strategy of shoot bagging of ears before silk emergence and ear exposure after 3-4 days
198 of tassel shedding was done. The plants that showed tassel maturity on the same day were tagged
199 and subsequently used for observation.

200 **Genotypic and gene expression data**

201 The genotypic data and other public datasets on various mapping populations used in this
202 study have been described previously (Khangura *et al.* 2019). Briefly, the public marker dataset

203 for IBM-RILs was obtained from MaizeGDB with 2,178 markers (Sen *et al.* 2010). The markers
204 were reduced to 2,156 after removing duplicate variants, with ~13.3 percent of missing data in the
205 final dataset. Expression data of *oy1* locus in IBM-RILs were obtained from a public repository of
206 the National Science Foundation grant (GEPR: Genomic Analyses of shoot meristem function in
207 maize; NSF DBI-0820610;
208 https://ftp.maizegdb.org/MaizeGDB/FTP/shoot_apical_meristem_data_scanlon_lab/). This data
209 consists of the expression of maize genes in the tissue derived from the shoot apex of 14 days old
210 IBM-RILs seedlings. The expression data from each gene is normalized to reads per kilobase of
211 transcript per million mapped reads (RPKM). Genotypic data consisting of 6611 SNPs for Syn10-
212 DH lines was obtained from Liu et al. 2015. This dataset had no missing genotypes and was used
213 as such for QTL analyses. Genotypes of the B73-Mo17 Near Isogenic Lines (BM-NILs) used for
214 QTL validation were obtained from Eichten *et al.* 2011.

215 **Molecular analyses**

216 OY1 sequencing: The genomic DNA and cDNA preparation derived from second and third fully-
217 expanded leaf of maize inbred lines were used to amplify the genic sequence of the *oy1* locus. The
218 detail description of methods and primers used for PCR amplification and sequence analyses of
219 the PCR products has been described previously (Khangura *et al.* 2019). Briefly, the PCR
220 amplicons were sequenced using Illumina and Sanger sequencing platforms at Purdue Genomic
221 Core Facility.

222 Allele-specific expression (ASE) assay: Three replications of B73-Mo17 near-isogenic lines
223 (BM-NILs) × *Oy1-N1989/oy1*:B73 F_1 progenies were grown in the field at Purdue Agronomy
224 Farm along with parental F_1 checks. Mutant siblings derived from four B73-like NIL crossed with
225 *Oy1-N1989/oy1*:B73 were selected for the ASE experiment. These NILs consisted of two B73-

226 like NILs with *vey1*^{Mo17}, and other two B73-NILs with *vey1*^{B73} genotype. Leaf tissue was harvested
227 from the top fully-expanded leaf at the V3 developmental stage from the mutant siblings of the
228 four B73-like NIL F_1 plots. For each biological replicate, tissue was pooled from 4-5 seedlings to
229 make one sample. The samples were stored at -80 ˚C until needed. The procedure of total RNA
230 isolation, cDNA synthesis, and the ASE assay has been described previously in detail (Khangura
231 *et al.* 2019). Briefly, total RNA was isolated using a modified Phenol/Lithium chloride protocol
232 (Eggermont et. al. 1996). One µg of DNase treated RNA was used to synthesize cDNA using
233 iScriptTM Select cDNA synthesis kit (catalog#170-8896, Bio-Rad, Hercules, CA) according to
234 the manufacturer's recommendations. The sensitivity of the ASE assay was tested using the
235 genomic DNA control that was prepared in the ratio of 1:1 (derived from B73 × Mo17 F_1 hybrid),
236 1:2, and 2:1 from B73 and Mo17 DNA. PCR was conducted using the forward oligonucleotide 5'-
237 TCACCGTCTGCAATGTCGCCGCTC -3' and reverse oligonucleotide 5'-
238 AGTATGCCCCTGTTGGCCTTGGCG -3' under following reaction conditions with 30 cycles of
239 polymerization (94˚C for 30s, 56˚C for 30s, 72 ˚C for 30s and final extension for 2 minutes) to
240 amplify the targeted region of OY1. The primer pair used in this assay flanked the SNP that causes
241 the L176F amino acid change that resulted in the *Oy1-N1989* mutant allele. PCR products were
242 sequenced on a MiSeq instrument (Illumina, San Diego, CA) at the Purdue Genomics Core Facility.
243 Allele count of the reads mapped to small reference sequence derived from B73 was done using
244 the GATK packages (DePristo *et al.* 2011). Read counts derived from GATK was used to calculate
245 allele-specific expression. As expected, control samples derived from genomic DNA displayed
246 bias in the read counts in a DNA dosage-dependent manner. Genomic DNA derived from B73 ×
247 Mo17 F_1 hybrids resulted in roughly 1:1 read counts demonstrating no bias in the assay.

248 **Statistical analyses**

249 The exploratory data analysis was done using JMP 13.0 (SAS Institute Inc. 2016). Averages of
250 various traits from line-cross populations, IBM-RILs and Syn10-DH, were subjected to QTL
251 analyses. QTL detection was done using a single interval mapping function "scanone" in R/qtl, a
252 software package implemented in R (Broman *et al.* 2003; R core Team 2013). Remarkably similar
253 results were obtained with composite interval mapping function "cim" in R/qtl (data not shown).
254 All the QTLs reported in this study are derived from "scanone" function.

255 **Defoliation assay**

256 The defoliation experiments were performed using maize inbred B73, sorghum (*Sorghum bicolor*)
257 inbred BTx623, and green foxtail (*Setaria viridis*) inbred A10.1. These experiments were
258 conducted under the greenhouse conditions using mogul base high-pressure sodium lamps (1000
259 Watts) as the supplemental light source for L:D cycle of 16:8 hours, with the temperature around
260 28ºC (day-time) and 20ºC (night-time). The maize inbred line B73 was defoliated at V3 leaf stage.
261 All the leaves were removed from the base, slightly above the ligule. Sorghum inbred BTx623
262 plants with three to four fully opened leaves (~20 days after sowing in the greenhouse) were
263 defoliated in a similar way. All fully expanded leaves at ~15 days after planting were removed in
264 *Setaria* plants. In addition, all tillers were also defoliated similar to the main stem in *Setaria*. The
265 flowering time was recorded on maize as described above. For sorghum and *Setaria*, the date of
266 head emergence on every plant was recorded, and it was deducted from the date of planting to
267 obtain days to heading.

268 **Non-structural carbohydrate (NSC) quantification**

269 The soluble sugars and starch were quantified from the mutant siblings of four B73-NILs × *Oy1-*
270 *N1989/oy1*:B73 F_1 population. Two of these NILs carried *vey1*^{Mo17}, while the other two had *vey1*^{B73}
271 genotype. Plants were grown in the field with three replications using RCBD. Top fully-expanded
272 leaf at the V3 stage was harvested at 1:00 PM and transferred to liquid nitrogen. Leaf tissues were
273 stored at -80°C until needed. Leaf samples were ground into a fine powder and ~100 mg of the
274 powder was used to extract sucrose, glucose, fructose, and starch using a previously described
275 method (Leach and Braun 2016). The quantification of these NSC was done using a method as
276 described (Leach *et al.* 2017). Briefly, high-performance anion exchange (HPAE) chromatography
277 (ICS-5000, Thermo-Fisher Scientific) was used to analyze the neutral fraction of the extract. The
278 HPAE chromatography equipped with a SA10 column was maintained at 45°C. An isocratic
279 potassium hydroxide solution (10 mmol/L) at a constant flow rate of 1.5mL/min^{-1} was used as an
280 eluent. Quadrupole wave form as per the manufacturer's recommendation was used for detection
281 with a disposable gold electrode maintained at 25°C. Sugar standards were used to construct a
282 standard curve, and samples were diluted to ensure that the detected values fell within the scope
283 of this curve.

284 **Gas-exchange measurements**

285 Gas-exchange measurements were taken on the field-grown plants during the summer of 2017 at
286 the Purdue ACRE farm. The gas-exchange measurements were taken on the third leaf on plants at
287 the V3 stage between 11 AM and 1 PM using LICOR LI-6400XT open photosynthesis system (LI-
288 COR Inc., Lincoln, NE, USA). Four B73-NILs × *Oy1-N1989/oy1*:B73, two with *vey1*^{Mo17}, were
289 used for these measurements. Plants were grown in a randomized complete block design of three

290 replicated blocks. For each genotype nine plants were measured as three replicates in each of the
291 three blocks. The following instrument conditions were maintained throughout the measurement
292 period: an artificial light source with an intensity of 1700 µmol photosynthetically active radiation
293 (PAR) m^{-2} s^{-1}, air temperature of ~31 ºC, CO_2 concentration of 400 mL L^{-1}, air flow of 400 µmol
294 s^{-1}, and relative humidity of 50-60%. Leaf temperatures varied from 32-34ºC during the
295 measurements.

296 Chlorophyll fluorescence measurements were taken on the same leaves used for gas-
297 exchange using a Handy PEA (Hansatech Instruments Ltd., Norfolk, UK). Leaves were dark-
298 adapted for 20-30 min using leaf clips before taking measurements. The saturation pulse rate of
299 3000 µmol m^{-2} s^{-1} was used to measure the emission of chlorophyll fluorescence. The initial
300 chlorophyll fluorescence yield (F_0), the variable chlorophyll fluorescence yield (F_v), and the
301 maximum chlorophyll fluorescence yield (F_m) were recorded. The maximum photochemical
302 efficiency of PSII in dark-adapted leaves was obtained by calculating the ratio of F_v/F_m.

303 **Data availability**

304 All phenotypic data from the QTL and NIL populations are attached to this manuscript as
305 supplemental tables S1-S3. All marker data was previously used in Khangura *et al.* 2019 and made
306 available to the public via Figshare (doi 10.25387/G3.7370948).

307 **Results**

308 **Negative affect of *Oy1-N1989* on flowering time is exacerbated by Mo17**

309 While preparing the material for our previous study (Khangura *et al.* 2019), we noticed that *Oy1-*
310 *N1989* exhibited a consistent delay in flowering. If this was due to variation in the accumulation

311 of chlorophyll, or downstream consequences of changes in chlorophyll content, we expect that
312 contribution of the *vey1* enhancing QTL from Mo17 should make this more severe. Heterozygous
313 *Oy1-N1989* mutant plants in the Mo17 × B73 hybrid genetic background flower up to two-weeks
314 later than wild-type siblings. The *Oy1-N1989* mutants also flower later in an isogenic inbred B73
315 background; however, the delay is less than half with mutants flowering four days after wild-type
316 siblings (Figure 1; Table S4). The wild-type B73 and Mo17 F_1 hybrid plants flower earlier than
317 the wild-type B73 inbred plants (Table S4). Maize is protandrous in nature; tassels mature earlier
318 than the ear-inflorescence. The effect of *Oy1-N1989* and *vey1* on flowering time was similar for
319 both anthesis and silk emergence. The window of difference in maturity of the tassel and ear
320 inflorescence, measured as ASI, is wider in the wild-type siblings compared to the mutants in
321 Mo17 × B73 hybrid background. However, the wild-type and mutant siblings are not different in
322 B73 inbred background. This is consistent with the *vey1* allele from Mo17 impacting all
323 phenotypes recorded for *Oy1-N1989* allele to date, including delayed flowering.

324 **Delayed flowering time of *Oy1-N1989* mutants in B73 × Mo17 mapping populations maps to**
325 ***vey1***

326 To test whether the effect in the hybrids was the result of the *vey1* locus, or some other factor in
327 the Mo17 background, we recording flowering time in wild-type and mutant plants of the F_1
328 progenies of *Oy1-N1989/oy1*:B73 pollen-parent with IBM-RILs and Syn10-DH. The crossing
329 scheme used for line-cross experiments have been described before (Khangura *et al.* 2019).
330 Hereafter, the hybrid populations developed from these crosses will be referred to as IBM-RILs
331 F_1 and Syn10-DH F_1 populations (Figure 2).

332 Pairwise correlations were calculated between previously reported chlorophyll index
333 measures (Khangura *et al.* 2019) and flowering time traits collected from the same plants (Tables

334 S5 and S6). The chlorophyll index was measured at two time points CCMI (25-30 days after
335 sowing) and CCMII (45-50 days after sowing). In both the IBM-RILs and Syn10-DH F_1
336 populations, significant positive correlations were observed between wild-type and mutant
337 flowering traits. In both populations, chlorophyll measurements in the wild-type siblings
338 (WT_CCMI and WT_CCMII) did not show any correlation with the mutant flowering time traits
339 (Figure 3, Table S5, and S6). In the IBM-RILs crosses, wild-type CCMII displayed a weak
340 significant negative correlation with wild-type DTA and DTS. Similarly, in the Syn10-DH crosses
341 wild-type CCMI displayed a significant weak negative correlation with wild-type DTA and DTS.
342 This indicates that the phenomena observed in our mutants, reduced chlorophyll content associated
343 with a delay in flowering time, could be seen in the wild-type siblings although the genetic basis
344 for the variation in wild-type chlorophyll was not resolved to the *oy1* locus (Khangura *et al.* 2019).
345 The most dramatic and obvious correlation were the negative correlation between CCM trait values
346 (CCMI and CCMII) and flowering time in the mutant siblings in both IBM-RILs and Syn10-DH
347 F_1 populations. The mutants in these populations also showed a clear increase in mean values for
348 days to anthesis and silking compared to wild-type siblings (Figure 4).

349 The frequency distribution plot of days to anthesis in mutant siblings of IBM-RILs and
350 Syn10-DH F_1 populations displayed a bimodal distribution, suggesting a single locus segregating
351 in these populations as the basis of flowering time suppression of *Oy1-N1989* mutants by B73
352 genotype (Figure 5). QTL mapping detected a single QTL on chromosome 10 at similar linkage
353 positions for all mutant derived flowering traits (Figure 5; Tables S7 and S8). This corresponds to
354 the *vey1* locus that we previously described as a major QTL that controls chlorophyll pigment
355 biosynthesis in the presence of the *Oy1-N1989* allele (Khangura *et al.* 2019). QTL mapping for
356 number of days to flower (anthesis and silking) in the mutant heterozygotes (MT_DTA and

357 MT_DTS), ratio of days to flower derived from mutant and wild-type siblings (Ratio_DTA and
358 Ratio_DTS), and the difference in days to flower between the wild-type and mutant siblings
359 (Diff_DTA and Diff_DTS) all detected *vey1* as the sole QTL in the population exceeding a
360 permutation-estimated significance threshold (alpha<0.05) in these traits and explaining ~40-48%
361 of the phenotypic variation in the IBM-RILs crosses, and >65% variation in the flowering traits in
362 Syn10-DH F_1 crosses. As expected, the *Oy1-N1989* enhancing $vey1^{Mo17}$ allele was associated with
363 a delay in flowering time in the mutant hybrid siblings (Tables S7 and S8). In addition to *vey1*, an
364 additional QTL controlling mutant anthesis and silking was detected in the Syn10-DH F_1
365 population on chromosome 2 which we call *other oy1 flowering time locus1* (*oof1*). This QTL
366 explained ~7-8% variation with the Mo17 allele at this locus resulting in ~2-3 days of delay in
367 reproductive maturity of mutant siblings.

368 Because of the very large effect of *vey1* on flowering time, and the mild segregation
369 distortion at this locus in both bi-parental populations (Khangura *et al.* 2019), weak QTL might be
370 detected by spurious linkage between chr2 and chr10 markers. To test this, we carried out multiple
371 regressions using top markers at *oof1* and *vey1* as independent variables and DTA in the Syn10-
372 DH as a dependent variable (data not shown). In this analysis, both *vey1* and *oof1* remained a
373 significant factor in the multiple regression and explained 62% and 2% of the variance in flowering
374 time, respectively. Inclusion of a *vey1* × *oof1* interaction term did not improve the fit of the model,
375 did not eliminate the significance of the *oof1* term, and the interaction term was not a significant
376 variable. Therefore, we propose that *oof1* is a novel QTL contingent upon the *Oy1-N1989* mutation
377 and genetically independent of *vey1*.

378 The mechanism(s) of the flowering time delays in *Oy1-N1989* mutants does not seem similar
379 to the effect of drought stress which differentially alters the time to silking and anthesis, commonly

380 measured by the anthesis-silking interval (ASI). The ASI of mutant and wild-type siblings were
381 not discernable and no QTL were detected for ASI in the mutants. In our conditions, we did not
382 detect any QTL for flowering time in wild-type siblings (Tables S7 and S8). Thus, detection of
383 *vey1* and *oof1* in these QTL analyses was conditioned on the presence of the *Oy1-N1989* allele
384 suggesting a role for either photosynthesis or chlorophyll metabolites in the regulation of flowering
385 time.

386 We further tested the effect of the *vey1* critical region using the BM-NIL F_1 population that
387 has been previously described. We observed that introgression of *vey1* locus from Mo17 resulted
388 in delaying flowering time in both B73 and Mo17 isogenic backgrounds, whereas *vey1*
389 introgression from B73 into Mo17 can restore the negative effect of Mo17 genotype at this position
390 on flowering time (Figure 6, Figure S3, and Table S3). No effect of *vey1* introgression from either
391 parent was visible on the flowering time of the wild-type siblings. Representative plants showing
392 the delayed reproductive maturity of B73-like NILs carrying $vey1^{Mo17}$, and reciprocal introgression
393 of $vey1^{B73}$ into Mo17 background displayed the opposite effect on flowering time (Figure 6). Thus,
394 these results clearly show the single locus effect of *vey1* on flowering time in maize in *Oy1-N1989*-
395 contingent manner in both isogenic inbred (B73) and hybrid (Mo17 × B73) background.

396 **Expression polymorphism in B73-like NILs is consistent with cis-acting regulatory**
397 **polymorphism at *vey1***

398 Our previous study looking at the suppression of *Oy1-N1989* mutant phenotype using chlorophyll
399 accumulation identified a cis-eQTL at *oy1* in the IBM-RILs population (Khangura *et al.* 2019).
400 Normalized expression (RPKM) of OY1 derived from 14 days old shoot apices of IBM-RILs (Li
401 et al., 2013; 2018) were used for this analysis. The top marker, isu085b, used in the detection of
402 this cis-eQTL was also one of the top significant markers for mutant flowering time traits (Figure

403 S1 and Table S9). Regression of OY1 RPKM and flowering traits collected in IBM-RILs F_1
404 population identified a significant linear relationship between gene expression in wild-type inbred
405 lines and flowering time measurements from mutant F_1 siblings (Figure S2 and Table S9). Roughly
406 21% of the variation in mutant DTA could be explained by OY1 expression in the IBM-RILs shoot
407 apices. OY1 RPKM did not predict variation in wild-type DTA.

408 The allele specific-expression (ASE) assay in our previous study identified bias in expression
409 with the wild-type *oy1* allele from Mo17 displaying relatively lower expression (Khangura *et al.*
410 2019). Our previous work compared mutant plants in two different genetic backgrounds which can
411 complicate the interpretations due to trans effect in the hybrid background. To overcome this
412 limitation, an ASE assay was designed to test bias at *oy1* using near-isogenic lines in the B73
413 background. These B73-like NILs consisted of two independent NILs with $vey1^{Mo17}$ introgression,
414 and two independent NILs with B73 genotype at *vey1*. This material was grown in the field and
415 expression of *oy1* was quantified in the top fully-expanded leaf at the V3 developmental stage.
416 Consistent with the previous ASE results, a significantly greater proportion of expression was
417 derived from the *Oy1-N1989* mutant allele when the wild-type *oy1* allele was contributed by
418 $vey1^{Mo17}$ introgression as compared to the isogenic mutant siblings carrying the wild-type *oy1*
419 allele from $vey1^{B73}$ locus (Table S10).

420 **Net CO_2 assimilation and sugar metabolism is reduced in *Oy1-N1989* mutants in *vey1*-**
421 **dependent manner**

422 We measured net CO_2 assimilation, sub-stomatal CO_2, photosystem II fluorescence, and
423 photosynthate accumulation in enhanced and suppressed *Oy1-N1989/oy1* mutants. A previous
424 study in maize has shown that reduction in chlorophyll levels in the leaves leads to a reduction in
425 photosynthetic rate (Huang *et al.* 2009). A similar reduction in photosynthetic rate should be

426 displayed by *Oy1-N1989/oy1* mutants and the Mo17 allele should show a greater reduction in
427 photosynthesis compared to the B73 allele. We tested this using F_1 progenies derived from four
428 B73-like NILs that were crossed to *Oy1-N1989/oy1*:B73 pollen. Two of these NILs had $vey1^{Mo17}$
429 introgression, whereas the other two had $vey1^{B73}$ genotype. The negative effect of $vey1^{Mo17}$
430 introgression on chlorophyll accumulation was visible in the *Oy1-N1989* mutant allele background
431 (Figure 6). As expected, photosynthetic rate (A) was reduced in mutants as compared to wild-type
432 siblings, and mutants were modified further by the *vey1* genotype (Table S11). Photosystem II
433 efficiency (Fv/Fm) measurements indicated higher photo-oxidative damage to the photosystem in
434 enhanced mutant plants compared to the suppressed mutants. Wild-type siblings of all four B73-
435 like NIL F_1 progenies showed no statistically significant difference for chlorophyll and gas-
436 exchange measurements. This indicates that, just as for chlorophyll content, the *vey1* QTL affects
437 net CO_2 assimilation in the presence of the *Oy1-N1989* mutant allele. No differences in stomatal
438 conductance (g_s) or transpiration (E) was observed in the mutant plants, however, severe mutant
439 plants showed significantly higher accumulation of intracellular CO_2 (Ci) compared to the
440 suppressed mutants suggesting the failure of the enhanced mutant plants to uptake carbon (Table
441 S11).

442 These differences in photosynthetic rate should result in a decrease of non-structural
443 carbohydrates. The levels of non-structural carbohydrates were determined from leaves of the
444 same mutant plants that were used for gas-exchange measurements. Levels of sucrose, glucose,
445 fructose, and starch were measured in these samples. All of these showed a significant reduction
446 in the enhanced mutants compared to the suppressed mutants in the B73 isogenic background
447 (Figure 7 and Table S12). Lower levels of sugars and starch in the enhanced mutants are consistent

448 with the observation of low photosynthetic rate in these genotypes compared to the suppressed
449 mutant NILs.

450 **Defoliation in *Zea mays*, *Sorghum bicolor*, and *Setaria viridis* delays flowering time**

451 The existing literature suggests sugars and carbohydrate metabolism play an important role in
452 regulating flowering time in plants (Ohto *et al.* 2001; Seo *et al.* 2011; Wahl *et al.* 2013). We
453 hypothesized that removal of source tissue should mimic sugar starvation observed in *Oy1-N1989*
454 mutants. As a result, defoliation should result in delayed flowering in defoliated (treated) plants
455 compared to non-defoliated (control) plants. We tested this hypothesis using the wild-type inbred
456 strains in maize and two other monocot species: *Sorghum bicolor* (sorghum) and *Setaria viridis*
457 (green foxtail). Each species was defoliated at an early vegetative stage when only a few leaves
458 had fully expanded. The intent was to deprive plants of leaf area and photosynthate early in
459 development to separate the loss of chlorophyll and the loss of photosynthate, which are coupled
460 in the *Oy1-N1989* mutant study. Defoliation delayed flowering in all the plant species tested
461 (Figure 8). Maize, sorghum, and green foxtail displayed a delay in flowering by about 13, 7, and
462 4 days, respectively, compared to the control plants. Therefore, based on the defoliation study in
463 multiple monocot species we propose that early season defoliation results in the removal of source
464 tissue that might be critical for vegetative to floral transition in plants. Surprisingly, one-week
465 post-defoliation, newly emerged leaves displayed a pale leaf color. Chlorophyll estimation using
466 CCM found a reduction in the leaf greenness in the defoliated treatments compared to the control
467 samples (Figure 8). The newly emerging leaves of maize, sorghum, and green foxtail showed
468 ~35%, ~48%, and ~58% reduction in chlorophyll, respectively, in the treated plants compared to
469 the control plants. Subsequent leaves emerging from the defoliated treatments displayed normal
470 leaf color suggesting recovery of the plants from defoliation stress. Thus, the delay in flowering

471 time is likely due to a loss of resources (carbon reserves) but cannot be formally distinguished
472 from a change in chlorophyll accumulation.

473 **Leaf senescence is suppressed by *Oy1-N1989* mutants in a *vey1*-dependent manner**

474 Leaf senescence can be induced in maize by sucrose accumulation in the leaves. This can be
475 accomplished genetically by disrupting sucrose transport (Braun *et al.* 2006; Baker and Braun
476 2008; Slewinski *et al.* 2009) or by preventing the maize ears from acting as a sink (Allison and
477 Weinmann 1970; Sekhon *et al.* 2012, 2019). In maize, previous studies have shown that leaf
478 senescence caused by pollination prevention or ear removal before pollination is genotype-
479 dependent (Ceppi et al. 1987; Allison and Weinmann 1970). We found that levels of free sugars
480 and starch were significantly lower in the young leaves of enhanced *Oy1-N1989* mutant B73 NILs
481 compared to the suppressed mutant NILs (Figure 8). If the accumulation of sugars in the leaves is
482 a pre-requisite for leaf senescence, we expected delayed senescence in the *Oy1-N1989* mutants
483 and for this to vary in a *vey1* dependent manner. We tested the effect of this differential sugar
484 accumulation in mutant B73-like NILs on induced leaf senescence by pollination avoidance. We
485 observed that 30 days-after-anthesis (DAA), the top leaves of the unpollinated wild-type B73
486 plants showed complete senescence of the leaves with only a few green patches. Unpollinated
487 *Oy1-N1989* mutant plants in the suppressed B73 NIL background did not show such an extreme
488 phenotype but rather, showed only a few patches of anthocyanin accumulation and cell death by
489 30 DAA (Figure 9). On the other hand, unpollinated mutant plants in B73 NIL background with
490 $vey1^{Mo17}$ introgression did not show any sign of leaf senescence at 30 DAA. At 42 DAA,
491 unpollinated wild-type and mutants with and without $vey1^{Mo17}$ genotype showed leaf senescence,
492 however, the enhancement of *Oy1-N1989* by the $vey1^{Mo17}$ resulted in substantially less cell death
493 and anthocyanin accumulation.

494 **Discussion**

495 Our previous work identified a modifier, *vey1*, that affects the chlorophyll accumulation in *Oy1-*
496 *N1989/oy1* heterozygotes (Khangura *et al.* 2019). The *vey1* polymorphism(s) are common natural
497 variant(s) linked to the *oy1* locus of maize. We proposed that *vey1* results from cis-acting
498 regulatory polymorphisms that affect the expression of OY1. The suppression of the mutant, and
499 accumulation of chlorophyll, follows the proportion of wild-type and mutant transcript levels
500 (Table S10 and Khangura *et al.* 2019). In this work, we describe a delay in flowering in the *Oy1-*
501 *N1989* mutants and demonstrate that *vey1* encodes a strong modifying QTL altering the flowering
502 time of mutant siblings in all mapping populations (Figures 5 and 6; Tables S7 and S8). Just as the
503 detection of *vey1* for CCM was contingent on *Oy1-N1989* mutant allele in the background, there
504 was no effect of *vey1* on flowering time in wild-type siblings. We observed the same marker,
505 isu085b, had the strongest effect on chlorophyll content, OY1 transcript abundance in shoot apices
506 (Khangura *et al.* 2019) and variation in flowering time of IBM-RILs x *Oy1-N1989* mutant F_1
507 mutant siblings (Table S9 and Figure S2). Taking these observations together, we propose that the
508 cis-acting eQTL at *oy1* is affecting chlorophyll level in *Oy1-N1989* mutants, and that the alteration
509 in photosynthesis through perturbed chlorophyll metabolism affects flowering time variation in
510 mutant siblings in these populations.

511 Our previous work on *vey1* has focused on the cryptic nature of the variation, and the
512 interaction between the *vey1* QTL and the *Oy1-N1989* mutant allele. However, the experiments
513 presented here clearly transcend this limitation and identify chlorophyll content as a heretofore
514 unappreciated correlate, if not determinant, of flowering time affecting even in wild-type siblings
515 (Figure 3; Tables S5 and S6). We observed that CCM values, especially CCMII in IBM-RILs and
516 CCMI in Syn10-DH F_1 populations, were negatively correlated with wild-type flowering time

517 measurements. This suggests a role for the normal variation in chlorophyll contents in the control
518 of flowering time in maize either via changes to photosynthetic output or signaling. As no QTL
519 were detected for CCM in the wild-type siblings in our previous work (Khangura *et al.* 2019), it
520 also suggests that mechanism responsible for CCM and flowering time covariation is likely
521 independent of *vey1*. This is further strengthened by the absence of an effect of *vey1* on flowering
522 time in the wild-type siblings in our NILs (Table S3 and Figure S3). It is possible that flowering
523 time QTL segregating in the B73 × Mo17 cross are fortuitously linked to other loci affecting CCM
524 in wild-type plants, which did not pass the threshold of detection in our QTL experiments.
525 Otherwise there should be no formal relationship between CCM and flowering time in other
526 populations with greater recombination or different alleles, such as in an association panel. Further
527 experiments are required to validate or reject the causal nature of the relationships between CCM
528 and flowering time in wild-type siblings of this material.

529 Even though Syn10-DH and IBM-RILs are derived from the same parents, they differ in the
530 method of development and rates of recombination (Liu et al. 2015; Hussain et al. 2007; Lee et al.
531 2002). Thus, these two populations yield different levels of resolution for QTL detection. Our
532 previous analysis to fine map *vey1* QTL using CCM values showed Syn10-DH to have a higher
533 mapping resolution than the IBM-RILs population (Khangura *et al.* 2019). We also observed
534 different QTL for flowering time in these populations. QTL analysis in Syn10-DH F_1 population
535 detected the *oof1* QTL on chromosome 2 affecting MT_DTA and MT_DTS as well as the major-
536 effect locus *vey1* (Table S8). The detection of *oof1* was dependent on the presence of the *Oy1-*
537 *N1989* mutant, but was neither contingent on nor displayed any epistatic interactions with *vey1* as
538 assessed by multiple regression. Thus, *oof1* appears to be a novel locus of independent mechanism
539 affecting flowering time in the *Oy1-N1989* mutants. This QTL on chromosome 2 was not detected

540 for any other trait in the Syn10-DH and IBM-RILs testcross populations with *Oy1-N1989/oy1*:B73
541 in the current study nor was it identified as a modifier of chlorophyll content in our previous study
542 (Khangura *et al.* 2019). The amount of phenotypic variation explained by *vey1* in flowering time
543 was higher in Syn10-DH experimental material than the IBM-RILs testcross population by ~20%
544 (Tables S7 and S8). Greater variation in flowering time in the IBM-RILs testcross progenies that
545 could not be modeled by marker genotypes may result from higher residual heterozygosity or
546 greater rates of pollen contamination during the single seed descent (SSD) procedure used to
547 generate the IBM-RILs (Lee et al. 2002). Heterozygosity is expected to be negligible in Syn10-
548 DH population because of the DH procedure employed to fix allele segregation during population
549 development (Hussain *et al.* 2007). In addition, we had a moderate increase in sample size in the
550 Syn10-DH (251 lines) as compared to the IBM-RILs (216 lines) that is expected to result in a
551 marginally greater power to detect QTL in the Syn10-DH F_1 populations.

552 Chlorophyll levels are correlated with the rate of photosynthesis in plants (Huang *et al.* 2009).
553 Some controversy has been reported in mutants of soybean affected in an ortholog of *oy1* with
554 some reports showing little impact on photosynthesis (Sakowska *et al.* 2018) and others clearly
555 demonstrating a linear relationship between chlorophyll variation and photosynthesis (Walker *et*
556 *al.* 2017). The reasons for conflicting conclusions results from soybean mutants are not fully clear
557 but it warrants some caution in making simplistic interpretations about the impact of chlorophyll
558 deficient mutants on photosynthesis. In our study, net CO_2 assimilation was associated with the
559 severity of the *Oy1-N1989* mutant phenotype. The effect of chlorophyll loss on CO_2 assimilation
560 measurements using a LICOR instrument was somewhat non-linear. A nearly 5-fold reduction in
561 CCM in *Oy1-N1989* NILs carrying a B73 allele at *vey1* resulted in in a 22% reduction in net CO_2
562 assimilation while the 10-fold reduction in CCM in *Oy1-N1989* NILs carrying a Mo17 allele at

563 *vey1* resulted in a 64% reduction in net photosynthetic rate, compared to their isogenic wild-type
564 siblings (Table S11). Ultimately, both reductions resulted in less accumulation of free sugars and
565 starch, with a substantially greater reduction in the enhanced mutant NILs (Figure 7; Tables S11
566 and S12).

567 The allelic interactions of *Oy1-N1989* and wild-type *oy1* alleles are consistent with the
568 inductive role of carbohydrate status on floral transition (Ohto et al. 2001; Seo et al. 2011; Wahl
569 et al. 2013; Minow et al. 2018). Additional work exploring proposed carbohydrate signaling
570 metabolites, such as T6P and organic acids, and analyses of the downstream floral integrators such
571 as the FT orthologs of maize are still needed to link our results to the existing models of floral
572 transition regulation in maize (Minow *et al.* 2018). One complexity that we observed in our data
573 is that the alternate experiments such as defoliation were not able to distinguish photosynthate
574 levels from changes in chlorophyll (Figure 8). The mechanical removal of leaves resulted in
575 changes to CCM. Two other subunits of magnesium chelatase are encoded by genes that were
576 identified in Arabidopsis as *genomes uncoupled* mutants, *gun4* and *gun5*, with altered retrograde,
577 plastid-to-nuclear, signaling with defects in chlorophyll metabolism (Susek *et al.* 1993; Mochizuki
578 *et al.* 2001; Larkin *et al.* 2003). Multiple studies have demonstrated retrograde signaling mutants
579 with defects in chlorophyll metabolism (Hernández-Verdeja and Strand 2018) and circadian
580 rhythm (Jones 2019). Retrograde signaling events are also associated with cell death, chloroplast
581 development, and etiolation but it acts via a number of modifiers of flowering, including
582 phytochromes, phytochrome signaling components, blue light perception via *crytochrome1,* and
583 circadian rhythmicity of key genes that affect flowering time. While retrograde signaling is an
584 attractive alternative model to sugar signaling for the phenomena reported here, mutants in
585 orthologs of *oy1* in both monocots and dicots (Mochizuki *et al.* 2001; Gadjieva *et al.* 2005) have

586 been tested for a *genomes uncoupled* phenotype and they did not perturb retrograde signaling. This
587 makes it unlikely that *Oy1-N1989* and *vey1* are altering flowering time via aberrant retrograde
588 signals. Additional experiments are necessary to clearly separate the effects of chlorophyll
589 metabolite levels from photosynthate levels to independently test their effects on flowering time
590 in maize.

591 We have known that defoliation is practiced in some maize nurseries to stagger flowering
592 time and permit intercrossing of lines with divergent reproductive maturities. We had presumed
593 that this was based on published research. Remarkably, we were not able to find a reference for
594 this practice. Previous work on defoliation in maize has looked at the effect of early and late season
595 defoliation on growth, and yield components but did not report flowering times (Crookston and
596 Hicks 1988; Pearson and Fletcher 2009). As a result, Figure 8 provides information that was
597 informally shared within the maize genetics research community but not described formally. In
598 addition, we extended this observation from maize to both sorghum and green foxtail, indicating
599 that defoliation can achieve staggered flowering times in these species as well. This may be a
600 general feature of grasses, but appears to not be universal in angiosperms as early-season
601 defoliation of photoperiod-sensitive strawberries did not affect flowering time (Guttridge 1959).
602 Surprisingly, the defoliation of maize, sorghum, and green foxtail resulted in reduced chlorophyll
603 accumulation in the new leaves. As a result, a mechanical treatment that was expected to only
604 affect photosynthetic leaf area, and not chlorophyll content, served to highlight the interconnected
605 nature of plant metabolism: large changes to any feature of central metabolism or plant physiology
606 result in large changes to all of central metabolism and plant physiology. Carefully conceived
607 narrow manipulation of the metabolites and additional studies of mechanisms of flowering time
608 modulation are required to determine how chlorophyll metabolism influences flowering time.

609 Sugar export and phloem loading mutants in maize that carry lesions in *tie-dyed1*, *tie-dyed2*,
610 *sucrose export defective1*, *psychedelic*, and *sucrose trasporter1* have all been shown to delay
611 flowering time (Braun *et al.* 2006; Baker and Braun 2008; Ma *et al.* 2008; Slewinski *et al.* 2009;
612 Slewinski and Braun 2010). We also observed declines in sugar levels in *Oy1-N1989* mutants
613 (Figure 7 and Table S12) and a delay in flowering time (Figure 1). It is tempting to consider these
614 mutants as a demonstration that sugar signaling can work independent of chlorophyll, but these
615 mutants also display low chlorophyll contents (Braun *et al.* 2006; Baker and Braun 2008; Ma *et*
616 *al.* 2008; Slewinski *et al.* 2009; Slewinski and Braun 2010). Curiously, *sucrose export defective1*
617 encodes tocopherol cyclase (Porfirova *et al.* 2002; Sattler *et al.* 2003). Tocopherol and chlorophyll
618 share the phytol side chain, and the salvage pathway for phytol side chains from chlorophyll can
619 contribute to tocopherol accumulation in both maize and Arabidopsis (Ischebeck *et al.* 2006;
620 Schelbert *et al.* 2009; Diepenbrock *et al.* 2017). While it is attractive to try and unify these findings,
621 chlorophyll breakdown products were only rate limiting for tocopherol synthesis in senescent
622 tissues of Arabidopsis (Zhang *et al.* 2014). Furthermore, in *Oy1-N1989* mutants the phytol
623 precursors should be abundant as this pool is not being consumed by chlorophyll biosynthesis.
624 Future experiments that more carefully explore these metabolites, for instance, via other mutants
625 that do not simultaneously affect multiple pathways are required. The finding that defoliation
626 impacts flowering time and the same biochemical and molecular responses as observed in the
627 photosynthetically compromised *Oy1-N1989* mutants may also provide mechanistic insights for
628 this phenomenon.

629 Accumulation of sugars in the leaves due to sink disruption has been proposed to induce leaf
630 senescence in a variety of angiosperms, including maize and Arabidopsis (Allison and Weinmann
631 1970; Ceppi *et al.* 1987; Pourtau *et al.* 2006; Sekhon *et al.* 2012, 2019). In maize, leaf senescence

632 is triggered when pollination is prevented and sucrose accumulates in leaves due to the lack of the
633 sink activity of a pollinated ear (Ceppi et al. 1987; Allison and Weinmann 1970). This sucrose-
634 dependent leaf senescence is genotype-dependent, and B73 is particularly susceptible to this
635 phenomenon. Genetic inheritance of the induced senescence phenomenon in maize inbred line
636 B73 is proposed to be under the control of a single dominant locus (Ceppi *et al.* 1987). The leaf
637 senescent phenotypes of the sucrose export mutants demonstrate that excessive photosynthate
638 accumulation can cause tissue to senesce regardless of ear presence (Braun *et al.* 2006; Baker and
639 Braun 2008; Ma *et al.* 2008; Slewinski *et al.* 2009). Induced leaf senescence by sink removal or
640 sugar application shows some overlap of biochemical and molecular mechanisms with natural
641 senescence in plants (summarized in Sekhon et al. 2012). A study of gene expression in the B73
642 inbred of maize identified senescence associated genes that exhibit gene expression changes during
643 pollination-prevented leaf senescence (Sekhon et al. 2012). We found that leaf senescence could
644 be prevented or delayed by the suppression of photosynthesis in the *Oy1-N1989* mutant and further
645 modulated by *vey1* variants. We expect that future gene expression studies in *Oy1-N1989* mutants
646 and sugar export mutants will identify genes consistently impacted by lower and higher
647 chlorophyll levels, presumably including senescence associated genes and genes regulating
648 carbohydrate metabolism.

649 **Conclusions**

650 Flowering time in plants is regulated by environmental and endogenous cues. In this study, we
651 demonstrate that the interaction between natural and induced variation at the *oy1* locus of maize,
652 encoding the magnesium chelatase subunit I responsible for the first committed step of chlorophyll
653 biosynthesis, regulates flowering time. The effect of *oy1* variation on flowering time and other

654 physiological traits is consistent with the previously proposed and widely-accepted role of
655 photosynthetically derived sugars on flowering time. The previously identified *vey1* QTL, a
656 putative cis-acting polymorphism(s) in the regulatory region proximal to *oy1*, modified the
657 flowering time delay in the *Oy1-N1989* mutant heterozygotes. Further, *vey1* and *Oy1-N1989*
658 affected gas-exchange parameters, chlorophyll fluorescence, sugar accumulation, and starch
659 accumulation in the immature leaves of *Oy1-N1989* mutant plants. Thus, all data are consistent
660 with *Oy1-N1989* altering flowering time by perturbing carbon fixation via photosynthesis.

661 **Acknowledgements**

662 We would like to thank the National Science Foundation for NSF grant 1444503 awarded to G.S.J.
663 and B.P.D which helped fund this research. We thank the Purdue ACRE and ICSC staff members
664 Mr. Jim Beaty and Mr. Jason Adams for help with planting, and management of the field
665 experiments described in this work. We also thank past Johal lab members for help with planting
666 and data collection. We would like to thank Mike Gosney for helping with gas-exchange
667 measurements. We gratefully acknowledge the bobcat operator for dumping loads of gravel on our
668 office walls while we attempted to write this paper. Solidarity with all.
669

670 **REFERENCES**

671 Abe, M., Y. Kobayashi, S. Yamamoto, Y. Daimon, A. Yamaguchi *et al.*, 2005 FD , a bZIP Protein
672 Mediating Signals from the Floral Pathway Integrator FT at the Shoot Apex. Science 309:
673 1052–1056.

674 Allison, J. C. S., and H. Weinmann, 1970a Effect of Absence of Developing Grain on and
675 Senescence of Maize Leaves. Plant Physiol. 46: 435–436.

676 Alter, P., S. Bircheneder, L.-Z. Zhou, U. Schlüter, M. Gahrtz *et al.*, 2016 Flowering Time-
677 Regulated Genes in Maize Include the Transcription Factor ZmMADS1. Plant Physiol. 172:
678 389–404.

679 Amasino, R. M., and S. D. Michaels, 2010 The Timing of Flowering. Plant Physiol. 154: 516–520.

680 Baker, R. F., and D. M. Braun, 2008 Tie-dyed2 functions with tie-dyed1 to promote carbohydrate
681 export from maize leaves. Plant Physiol. 146: 1085–1097.

682 Bomblies, K., R.-L. Wang, B. A. Ambrose, R. J. Schmidt, R. B. Meeley *et al.*, 2003 Duplicate
683 FLORICAULA/LEAFY homologs zfl1 and zfl2 control inflorescence architecture and flower
684 patterning in maize. Development 130: 2385–2395.

685 Bouchet, S., P. Bertin, T. Presterl, P. Jamin, D. Coubriche *et al.*, 2017 Association mapping for
686 phenology and plant architecture in maize shows higher power for developmental traits
687 compared with growth influenced traits. Heredity (Edinb). 118: 249–259.

688 Braun, D. M., Y. Ma, N. Inada, M. G. Muszynski, and R. F. Baker, 2006 tie-dyed1 Regulates
689 carbohydrate accumulation in maize leaves. Plant Physiol. 142: 1511–22.

690 Broman, K. W., H. Wu, S. Sen, and G. a. Churchill, 2003 R/qtl: QTL mapping in experimental
691 crosses. Bioinformatics 19: 889–890.

692 Buckler, E. S., J. B. Holland, P. J. Bradbury, C. B. Acharya, P. J. Brown *et al.*, 2009 The genetic
693 architecture of maize flowering time. Science 325: 714–718.

694 Ceppi, D., M. Sala, E. Gentinetta, A. Verderio, and M. Motto, 1987 Genotype-Dependent Leaf
695 Senescence in Maize INHERITANCE AND EFFECTS OF POLLINATION-PREVENTION.
696 Plant Physiol. 85: 720–725.

697 Chen, M., J. Chory, and C. Fankhauser, 2004 Light Signal Transduction in Higher Plants. Annu.
698 Rev. Genet. 38: 87–117.

699 Cho, L. H., R. Pasriga, J. Yoon, J. S. Jeon, and G. An, 2018 Roles of Sugars in Controlling
700 Flowering Time. J. Plant Biol. 61: 121–130.

701 Cho, L. H., J. Yoon, and G. An, 2017 The control of flowering time by environmental factors.
702 Plant J. 90: 708–719.

703 Colasanti, J., Z. Yuan, and V. Sundaresan, 1998 The indeterminate gene encodes a zinc finger
704 protein and regulates a leaf-generated signal required for thetransition to flowering in maize.
705 Cell 93: 593–603.

706 Coles, N. D., M. D. McMullen, P. J. Balint-Kurti, R. C. Pratt, and J. B. Holland, 2010 Genetic

control of photoperiod sensitivity in maize revealed by joint multiple population analysis. Genetics 184: 799–812.

Coneva, V., D. Guevara, S. J. Rothstein, and J. Colasanti, 2012 Transcript and metabolite signature of maize source leaves suggests a link between transitory starch to sucrose balance and the autonomous floral transition. J. Exp. Bot. 63: 5079–5092.

Coneva, V., T. Zhu, and J. Colasanti, 2007 Expression differences between normal and indeterminate1 maize suggest downstream targets of ID1, a floral transition regulator in maize. J. Exp. Bot. 58: 3679–3693.

Corbesier, L., P. Lejeune, and G. Bernier, 1998 The role of carbohydrates in the induction of flowering in Arabidopsis thaliana: Comparison between the wild type and a starchless mutant. Planta 206: 131–137.

Corbesier, L., C. Vincent, S. Jang, F. Fornara, Q. Fan *et al.*, 2007 FT protein movement contributes to long-distance signaling in floral induction of Arabidopsis. Science 316: 1030–1033.

Crookston, R. K., and D. R. Hicks, 1988 Effect of Early Defoliation on Maize Growth and Yield: an Eleven-year Perspective. Crop Sci. 28: 371–373.

Danilevskaya, O. N., X. Meng, D. A. Selinger, S. Deschamps, P. Hermon *et al.*, 2008 Involvement of the MADS-Box Gene ZMM4 in Floral Induction and Inflorescence Development in Maize. Plant Physiol. 147: 2054–2069.

DePristo, M. A., E. Banks, R. Poplin, K. V Garimella, J. R. Maguire *et al.*, 2011 A framework for variation discovery and genotyping using next-generation DNA sequencing data. Nat. Genet. 43: 491–498.

Diepenbrock, C. H., C. B. Kandianis, A. E. Lipka, M. Magallanes-Lundback, B. Vaillancourt *et al.*, 2017 Novel Loci Underlie Natural Variation in Vitamin E Levels in Maize Grain. Plant Cell 29: 2374–2392.

Doebley, J., A. Stec, and L. Hubbard, 1997 The evolution of apical dominance in maize. Nature 386: 485–488.

Eichten, S. R., J. M. Foerster, N. de Leon, Y. Kai, C.-T. Yeh *et al.*, 2011 B73-Mo17 near-isogenic lines demonstrate dispersed structural variation in maize. Plant Physiol. 156: 1679–90.

Evans, M. M., and R. S. Poethig, 1995 Gibberellins promote vegetative phase change and reproductive maturity in maize. Plant Physiol. 108: 475–87.

Eveland, A. L., and D. P. Jackson, 2012 Sugars, signalling, and plant development. J. Exp. Bot. 63: 3367–3377.

Gadjieva, R., E. Axelsson, U. Olsson, and M. Hansson, 2005 Analysis of gun phenotype in barley magnesium chelatase and Mg-protoporphyrin IX monomethyl ester cyclase mutants. Plant Physiol. Biochem. 43: 901–908.

Gibson, L. C. D., R. D. Willows, C. G. Kannangara, D. von Wettstein, and C. N. Hunter, 1995 Magnesium-protoporphyrin chelatase of Rhodobacter sphaeroides: reconstitution of activity by combining the products of the bchH, -I, and -D genes expressed in Escherichia coli. Proc. Natl. Acad. Sci. U. S. A. 92: 1941–1944.

Guttridge, C. G., 1959 Evidence for a Flower Inhibitor and Vegetative Growth Promoter in the

Strawberry. Ann. Bot. 23: 351–360.

Hernández-Verdeja, T., and Å. Strand, 2018 Retrograde Signals Navigate the Path to Chloroplast Development. Plant Physiol. 176: 967–976.

Huang, M., T. L. Slewinski, R. F. Baker, D. Janick-Buckner, B. Buckner *et al.*, 2009 Camouflage patterning in maize leaves results from a defect in porphobilinogen deaminase. Mol. Plant 2: 773–89.

Huang, C., H. Sun, D. Xu, Q. Chen, Y. Liang *et al.*, 2017 ZmCCT9 enhances maize adaptation to higher latitudes. Proc. Natl. Acad. Sci. 115: E334–E341.

Hung, H.-Y., L. M. Shannon, F. Tian, P. J. Bradbury, C. Chen *et al.*, 2012 ZmCCT and the genetic basis of day-length adaptation underlying the postdomestication spread of maize. Proc. Natl. Acad. Sci. 109: E1913–E1921.

Hussain, T., P. Tausend, G. Graham, and J. Ho, 2007 Registration of IBM2 SYN10 Doubled Haploid Mapping Population of Maize. J. Plant Regist. 1: 81.

Ischebeck, T., A. M. Zbierzak, M. Kanwischer, and P. Dörmann, 2006 A salvage pathway for phytol metabolism in Arabidopsis. J. Biol. Chem. 281: 2470–2477.

Jones, M. A., 2019 Retrograde signalling as an informant of circadian timing. New Phytol. 221: 1749–1753.

Karl, J., 2016 Maize Leafy1 45ft. Maize Genet. Coop. Newsl. 90: 1–15.

Khangura, R. S., S. Marla, B. P. Venkata, N. J. Heller, G. S. Johal *et al.*, 2019 A Very Oil Yellow1 Modifier of the Oil Yellow1-N1989 Allele Uncovers a Cryptic Phenotypic Impact of Cis-regulatory Variation in Maize. G3 9: 375–390.

Kozaki, A., S. Hake, and J. Colasanti, 2004 The maize ID1 flowering time regulator is a zinc finger protein with novel DNA binding properties. Nucleic Acids Res. 32: 1710–1720.

Lang, A., 1952 Physiology of Flowering. Ann. Rev. Plant. Physiol. 3: 265–306.

Lang, A., 1957 The effect of gibberellin upon flower formation. Proc. Natl. Acad. Sci. 43: 709–717.

Larkin, R. M., J. M. Alonso, J. R. Ecker, and J. Chory, 2003 GUN4, a regulator of chlorophyll synthesis and intracellular signaling. Science 299: 902–906.

Leach, K. A., and D. M. Braun, 2016 Soluble Sugar and Starch Extraction and Quantification from Maize (*Zea mays*) Leaves. Curr. Protoc. Plant Biol. 1: 139–161.

Leach, K. A., T. M. Tran, T. L. Slewinski, R. B. Meeley, and D. M. Braun, 2017 Sucrose transporter2 contributes to maize growth, development, and crop yield. J. Integr. Plant Biol. 59: 390–408.

Lee, M., N. Sharopova, W. D. Beavis, D. Grant, M. Katt *et al.*, 2002 Expanding the genetic map of maize with the intermated B73 x Mo17 (IBM) population. Plant Mol. Biol. 48: 453–61.

Liang, Y., Q. Liu, X. Wang, C. Huang, G. Xu *et al.*, 2019 ZmMADS69 functions as a flowering activator through the ZmRap2.7-ZCN8 regulatory module and contributes to maize flowering time adaptation. New Phytol. 221: 2335–2347.

Liu, H., Y. Niu, P. J. Gonzalez-Portilla, H. Zhou, L. Wang *et al.*, 2015 An ultra-high-density map

786 as a community resource for discerning the genetic basis of quantitative traits in maize. BMC
787 Genomics 16: 1078.

788 Ma, Y., R. F. Baker, M. Magallanes-Lundback, D. Dellapenna, and D. M. Braun, 2008 Tie-dyed1
789 and Sucrose export defective1 act independently to promote carbohydrate export from maize
790 leaves. Planta 227: 527–538.

791 Meng, X., M. G. Muszynski, and O. N. Danilevskaya, 2011 The FT-Like ZCN8 Gene Functions
792 as a Floral Activator and Is Involved in Photoperiod Sensitivity in Maize. Plant Cell 23: 942–
793 960.

794 Minow, M. A. A., L. M. Ávila, K. Turner, E. Ponzoni, I. Mascheretti *et al.*, 2018 Distinct gene
795 networks modulate floral induction of autonomous maize and photoperiod-dependent teosinte.
796 J. Exp. Bot. 69: 2937–2952.

797 Mochizuki, N., J. a Brusslan, R. Larkin, a Nagatani, and J. Chory, 2001 Arabidopsis genomes
798 uncoupled 5 (GUN5) mutant reveals the involvement of Mg-chelatase H subunit in plastid-
799 to-nucleus signal transduction. Proc. Natl. Acad. Sci. U. S. A. 98: 2053–2058.

800 Moghaddam, M. R. B., and W. Van den Ende, 2013 Sugars, the clock and transition to flowering.
801 Front. Plant Sci. 4: 1–6.

802 Muszynski, M. G., T. Dam, B. Li, D. M. Shirbroun, Z. Hou *et al.*, 2006 delayed flowering1
803 Encodes a basic leucine zipper protein that mediates floral inductive signals at the shoot apex
804 in maize. Plant Physiol. 142: 1523–1536.

805 Mutasa-Göttgens, E., and P. Hedden, 2009 Gibberellin as a factor in floral regulatory networks. J.
806 Exp. Bot. 60: 1979–1989.

807 Ohto, M.-A., K. Onai, Y. Furukawa, E. Aoki, T. Araki *et al.*, 2001 Effects of Sugar on Vegetative
808 Development and Floral Transition in Arabidopsis. Plant Physiol. 127: 252–261.

809 Paul, M. J., 2008 Trehalose 6-phosphate: a signal of sucrose status. Biochem. J. 412: 1–2.

810 Pearson, A., and A. L. Fletcher, 2009 Effect of total defoliation on maize growth and yield. Agron.
811 New Zeal. 39: 1–6.

812 Porfirova, S., E. Bergmuller, S. Tropf, R. Lemke, and P. Dormann, 2002 Isolation of an
813 Arabidopsis mutant lacking vitamin E and identification of a cyclase essential for all
814 tocopherol biosynthesis. Proc. Natl. Acad. Sci. 99: 12495–12500.

815 Pourtau, N., R. Jennings, E. Pelzer, J. Pallas, and A. Wingler, 2006 Effect of sugar-induced
816 senescence on gene expression and implications for the regulation of senescence in
817 Arabidopsis. Planta 224: 556–568.

818 R core Team, 2013 R: A language and environment for statistical computing. R Foundation for
819 Statistical Computing, Vienna, Austria. ISBN 3-900051-07-0, http://www.R-project.org/.

820 Sakowska, K., G. Alberti, L. Genesio, A. Peressotti, G. Delle Vedove *et al.*, 2018 Leaf and canopy
821 photosynthesis of a chlorophyll deficient soybean mutant. Plant Cell Environ. 41: 1427–1437.

822 Salvi, S., G. Sponza, M. Morgante, D. Tomes, X. Niu *et al.*, 2007 Conserved noncoding genomic
823 sequences associated with a flowering-time quantitative trait locus in maize. Proc. Natl. Acad.
824 Sci. U. S. A. 104: 11376–11381.

825 Samach, A., H. Onouchi, S. E. Gold, G. S. Ditta, Z. Schwarz- *et al.*, 2000 Distinct Roles of

826 CONSTANS Target Genes in Reproductive Development of Arabidopsis. Science 288:
827 1613–1616.

828 Sattler, S. E., E. B. Cahoon, S. J. Coughlan, and D. Dellapenna, 2003 Characterization of
829 Tocopherol Cyclases from Higher Plants and Cyanobacteria . Evolutionary Implications for
830 Tocopherol Synthesis and Function. Plant Physiol. 132: 2184–2195.

831 Sawers, R. J. H., J. Viney, P. R. Farmer, R. R. Bussey, G. Olsefski *et al.*, 2006 The maize Oil
832 yellow1 (Oy1) gene encodes the I subunit of magnesium chelatase. Plant Mol. Biol. 60: 95–
833 106.

834 Schelbert, S., S. Aubry, B. Burla, B. Agne, F. Kessler *et al.*, 2009 Pheophytin Pheophorbide
835 Hydrolase (Pheophytinase) Is Involved in Chlorophyll Breakdown during Leaf Senescence
836 in Arabidopsis. Plant Cell 21: 767–785.

837 Searle, N. E., 1965 Physiology of Flowering. Ann. Rev. Plant. Physiol. 16: 97–118.

838 Sekhon, R. S., K. L. Childs, N. Santoro, C. E. Foster, C. R. Buell *et al.*, 2012 Transcriptional and
839 Metabolic Analysis of Senescence Induced by Preventing Pollination in Maize. Plant Physiol.
840 159: 1730–1744.

841 Sekhon, R. S., C. Saski, R. Kumar, B. Flinn, F. Luo *et al.*, 2019 Integrated Genome-Scale Analysis
842 Identifies Novel Genes and Networks Underlying Senescence in Maize. Plant Cell
843 tpc.00930.2018.

844 Sen, T. Z., L. C. Harper, M. L. Schaeffer, C. M. Andorf, T. E. Seigfried *et al.*, 2010 Choosing a
845 genome browser for a Model Organism Database: surveying the Maize community. Database
846 2010: 1–9.

847 Seo, P. J., J. Ryu, S. K. Kang, and C. M. Park, 2011 Modulation of sugar metabolism by an
848 INDETERMINATE DOMAIN transcription factor contributes to photoperiodic flowering in
849 Arabidopsis. Plant J. 65: 418–429.

850 Slewinski, T. L., and D. M. Braun, 2010 The Psychedelic genes of maize redundantly promote
851 carbohydrate export from leaves. Genetics 185: 221–232.

852 Slewinski, T. L., A. Garg, G. S. Johal, and D. M. Braun, 2010 Maize SUT1 functions in phloem
853 loading. Plant Signal. Behav. 5: 1–4.

854 Slewinski, T. L., R. Meeley, and D. M. Braun, 2009 Sucrose transporter1 functions in phloem
855 loading in maize leaves. J. Exp. Bot. 60: 881–892.

856 Steinhoff, J., W. Liu, J. C. Reif, G. Della Porta, N. Ranc *et al.*, 2012 Detection of QTL for
857 flowering time in multiple families of elite maize. Theor. Appl. Genet. 125:.

858 Susek, R. E., F. M. Ausubel, and J. Chory, 1993 Signal Transduction Mutants of Arabidopsis
859 Uncouple Nuclear CAB and RBCS Gene Expression from Chloroplast Development. Cell 74:
860 787–799.

861 Swarts, K., R. M. Gutaker, B. Benz, M. Blake, R. Bukowski *et al.*, 2017 Genomic estimation of
862 complex traits reveals ancient maize adaptation to temperate North America. Science 357:
863 512–515.

864 Vega, S. H., M. Sauer, J. A. J. Orkwiszewski, and S. Poethig, 2002 The early phase change gene
865 in Maize. Plant Cell 14: 133–147.

866 Wahl, V., J. Ponnu, A. Schlereth, S. Arrivault, T. Langenecker *et al.*, 2013 Regulation of flowering
867 by Trehalose-6-phosphate signalling in Arabidopsis thaliana. Science 339: 704–708.

868 Walker, B. J., D. T. Drewry, R. A. Slattery, A. VanLoocke, Y. B. Cho *et al.*, 2017 Chlorophyll can
869 be reduced in crop canopies with little penalty to photosynthesis. Plant Physiol. 176: 1215–
870 1232.

871 Walker, C. J., and J. D. Weinstein, 1991 In vitro assay of the chlorophyll biosynthetic enzyme Mg-
872 chelatase: resolution of the activity into soluble and membrane-bound fractions. Proc. Natl.
873 Acad. Sci. U. S. A. 88: 5789–5793.

874 Wang, R. L., A. Stec, J. Hey, L. Lukens, and J. Doebley, 1999 The limits of selection during maize
875 domestication. Nature 398: 236–239.

876 Wigge, P. A., M. C. Kim, K. E. Jaeger, W. Busch, M. Schmid *et al.*, 2005 Integration of Spatial
877 and Temporal Information During Floral Induction in Arabidopsis. Science 309: 1056–1059.

878 Zeevaart, J. A. D., 1962 Physiology of Flowering. Science 137: 723–731.

879 Zhang, W., T. Liu, G. Ren, S. Hörtensteiner, Y. Zhou *et al.*, 2014 Chlorophyll Degradation: The
880 Tocopherol Biosynthesis-Related Phytol Hydrolase in Arabidopsis Seeds Is Still Missing.
881 Plant Physiol. 166: 70–79.

882 Zhang, L., H. Yu, S. Lin, and Y. Gao, 2016 Molecular Characterization of FT and FD Homologs
883 from Eriobotrya deflexa Nakai forma koshunensis. Front. Plant Sci. 7: 1–10.

884

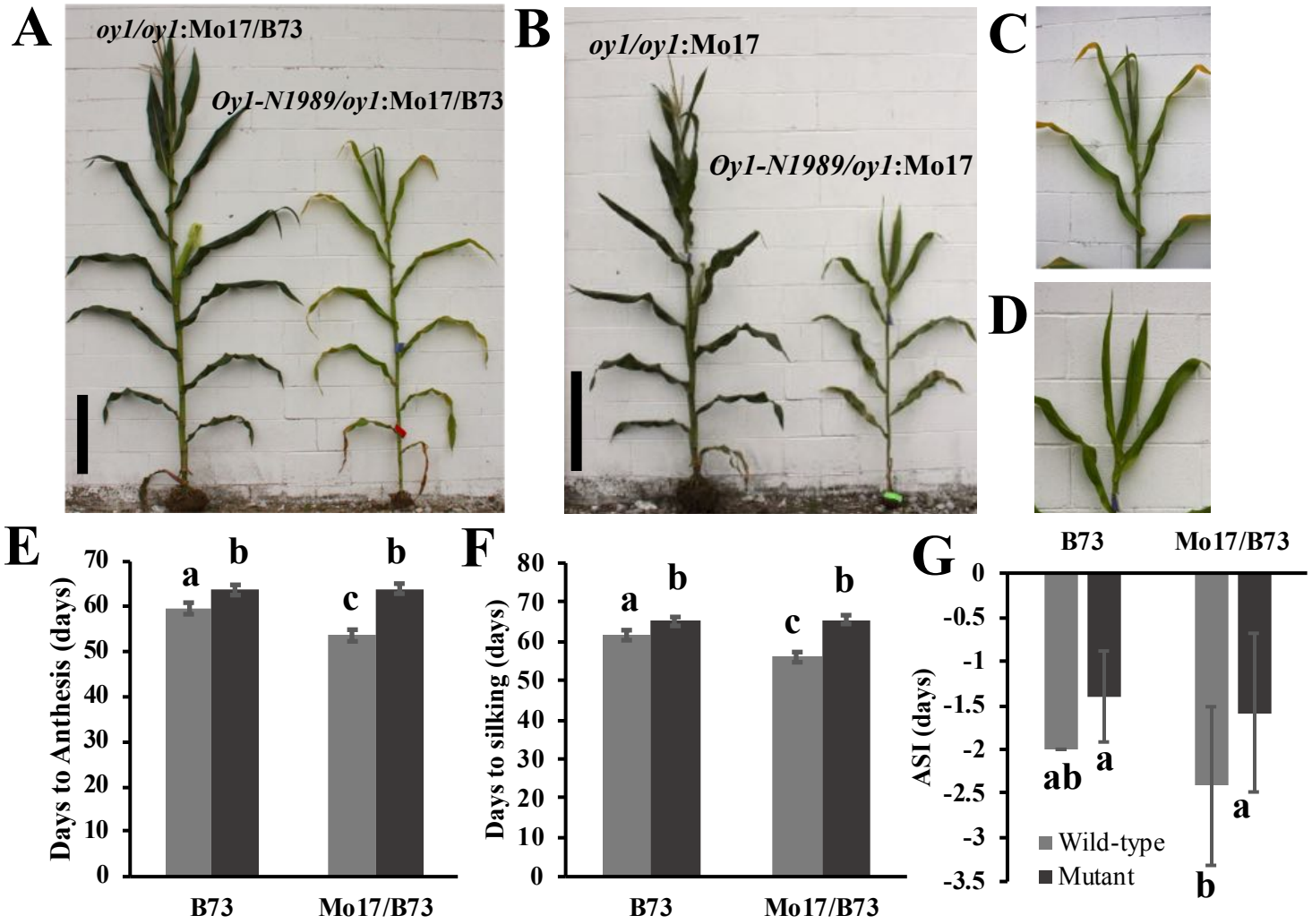

Figure 1. Reproductive maturity is delayed by *Oy1-N1989* allele in maize (A) Wild-type (left) and mutant (right) sibling from Mo17 x *Oy1-N1989/oy1*:B73 cross (reproduced from Figure 1b from Khangura *et. al*., 2019), black scale bar = 50 cm. (B) Wild-type (left) and mutant (right) sibling from Mo17 x *Oy1-N1989/oy1*:Mo17 cross. Close-up view of the emerging tassel of mutant siblings (C) from panel A, and (D) from panel B. Distribution of (E) days to anthesis, (F) days to silking, and (G) Anthesis-silking interval (ASI) in the wild-type and mutant siblings in B73 and Mo17 x B73 (Mo17/B73) hybrid genetic backgrounds.

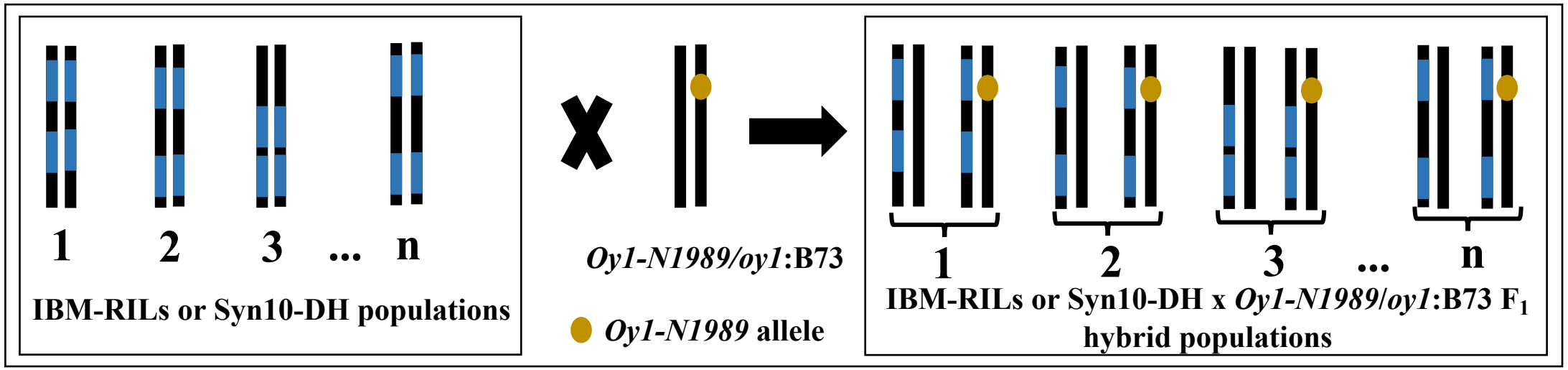

Figure 2. Crossing scheme to map *Oy1-N1989* enhancer/suppressor loci using IBM-RILs (n=216) and Syn10-DH (n=251) populations. Black and blue colors indicate B73 and Mo17 genotypes. Chromosome 10 of the heterozygous pollen parent *Oy1-N1989/+*:B73 is shown with a golden spot indicating *Oy1-N1989* mutant allele. The resulting F_1 progenies from these crosses are depicted here with state of chromosome 10 for each F_1 testcross showing segregation of wildtype and mutant (with the golden spot) siblings.

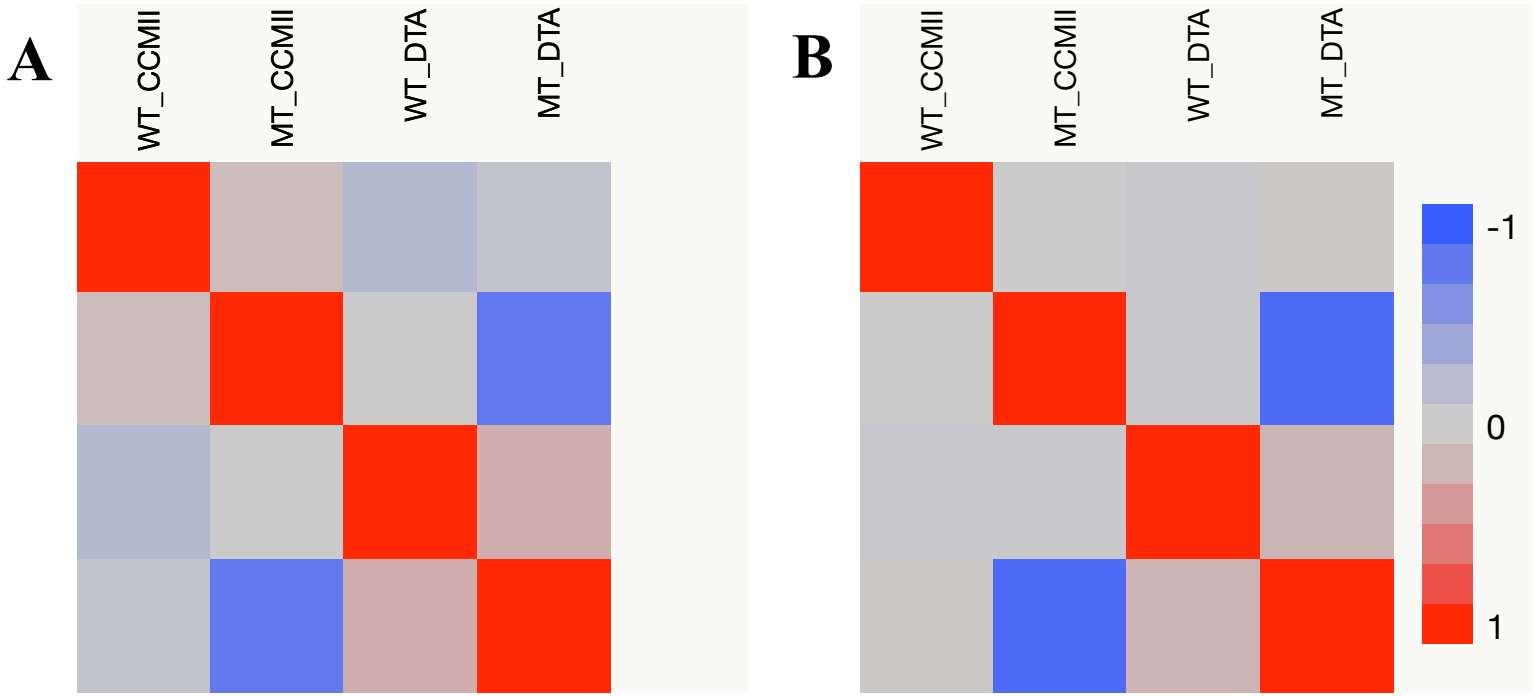

Figure 3. Pairwise correlation matrix between wildtype CCMII (WT_CCMII), mutant CCMII (MT_CCMII), wildtype days to anthesis (WT_DTA), and mutant days to anthesis (MT_DTA) in (A) IBM-RILs x *Oy1-N1989/oy1*:B73, and (B) Syn10-DH x *Oy1-N1989/oy1*:B73 F_1 test cross populations.

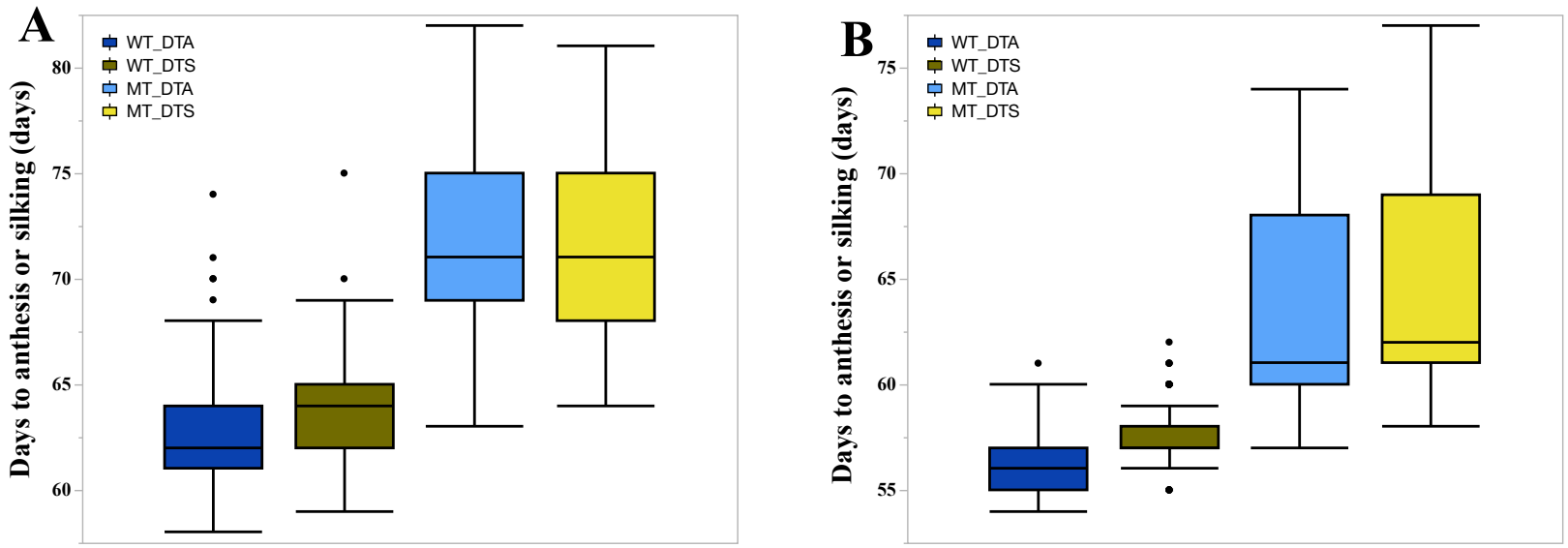

Figure 4. Distribution of days to flower (anthesis and silking) in the wildtype and mutant siblings in (A) IBM-RILs x *Oy1-N1989/oy1*:B73, and (B) Syn10-DH x *Oy1-N1989/oy1*:B73 F_1 test cross populations. Abbreviations: wildtype days to anthesis (WT_DTA), wildtype days to silking (WT_DTS), mutant days to anthesis (MT_DTA), and mutant days to silking (DTS).

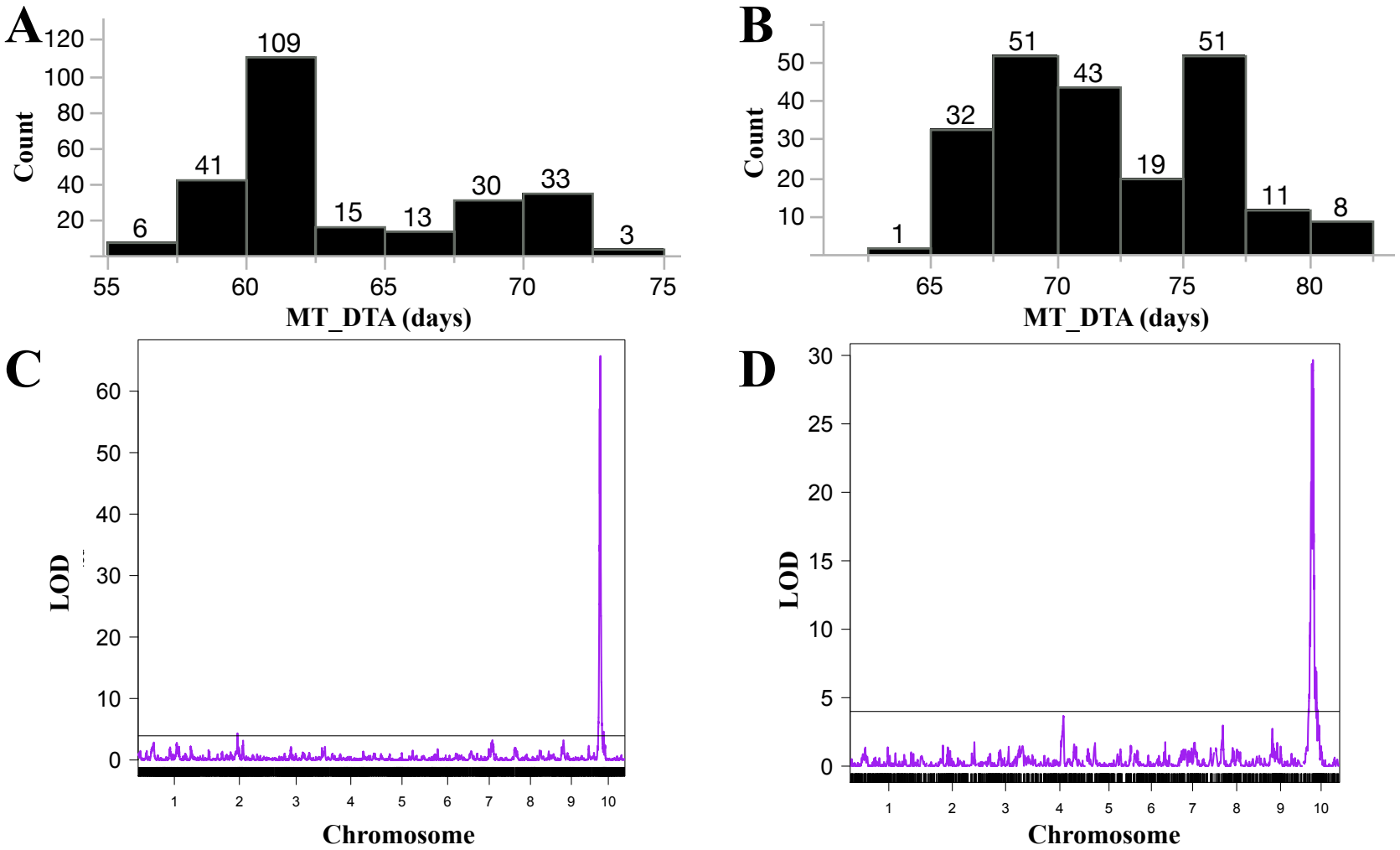

Figure 5. Distribution of days to 50% anthesis of the mutant siblings (MT_DTA) in (A) Syn10-DH x *Oy1-N1989/oy1*:B73, and (B) IBM-RILs x *Oy1-N1989/oy1*:B73 F_1 population. Genome wide QTL plot of MT_DTA in (C) Syn10-DH, and (D) IBM-RILs F_1 population. X-axis indicates the chromosome number and Y-axis indicates the logarithm of odds (LOD) of tested markers. Black horizontal bar indicates permutation testing based threshold for QTL detection.

Figure 6. Effect of *vey1* locus from B73 and Mo17 on flowering time in reciprocal isogenic backgrounds
(A) Delayed maturity of the heterozygous mutants in isogenic Mo17 (BC_7 generation) inbred background, compared to the wildtype siblings. Mutant and wildtype siblings in b030 (B73-like NIL with $vey1^{B73}$) shows early flowering while the isogenic B73 introgression of the $vey1^{Mo17}$ locus in b094 exhibits delayed flowering.
(B) Early maturity in the heterozygous mutant in m097 (Mo17-like NIL with $vey1^{B73}$) compared to the mutant in B73 x Mo17 F_1 hybrid background. Measuring stick on the left in both panels is 243 cm.

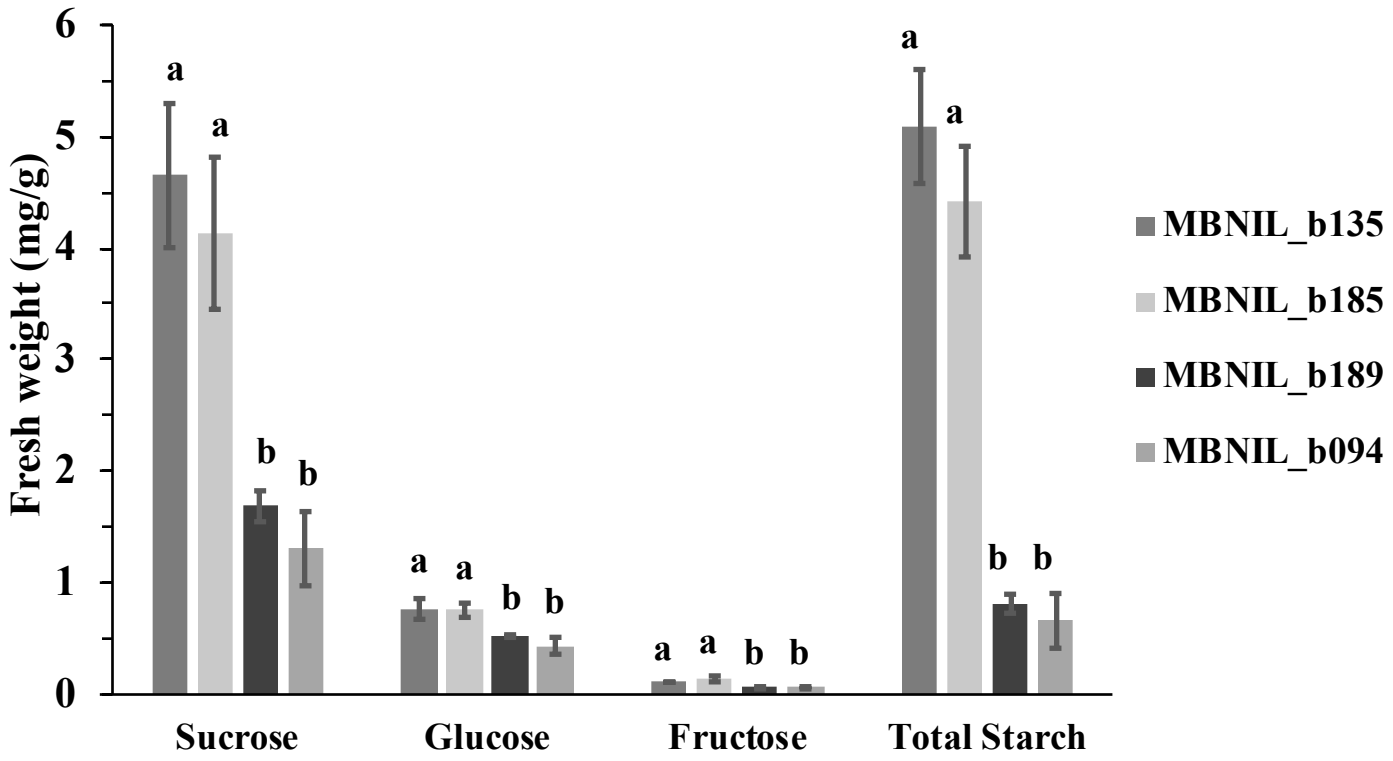

Figure 7. Effect of *vey1* on leaf soluble sugars and starch content in *Oy1-N1989/oy1* heterozygotes in the isogenic B73 NILs. NILs b135, and b185 have *vey1*^{B73} introgression, whereas b189, and b094 have *vey1*^{Mo17} introgression.

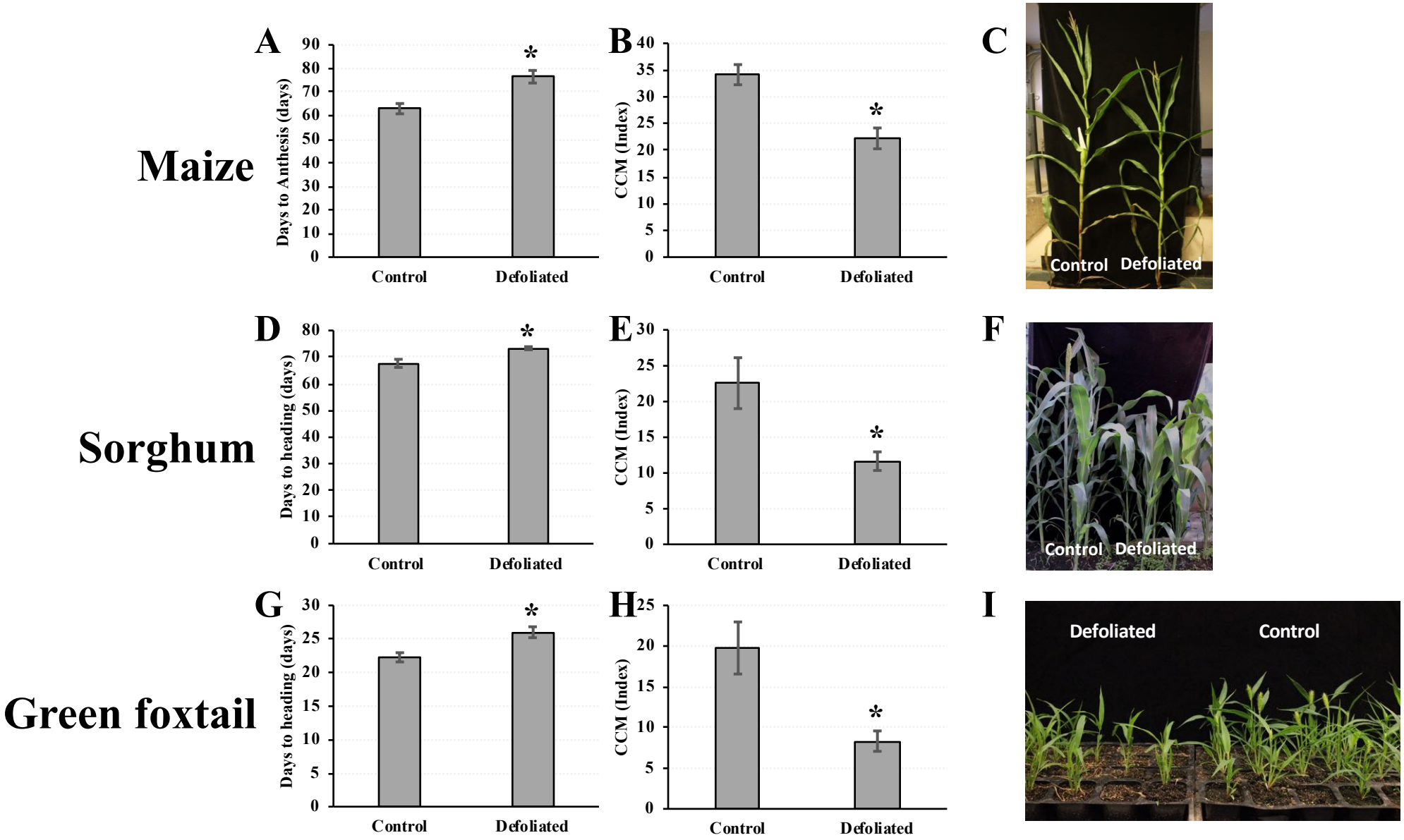

Figure 8. Effect of defoliation on flowering time and leaf color in (A-C) maize, (D-F) sorghum, and (G-I) green foxtail. Asterisk indicates significant difference between treatment means using student's t-test at $p<0.05$.

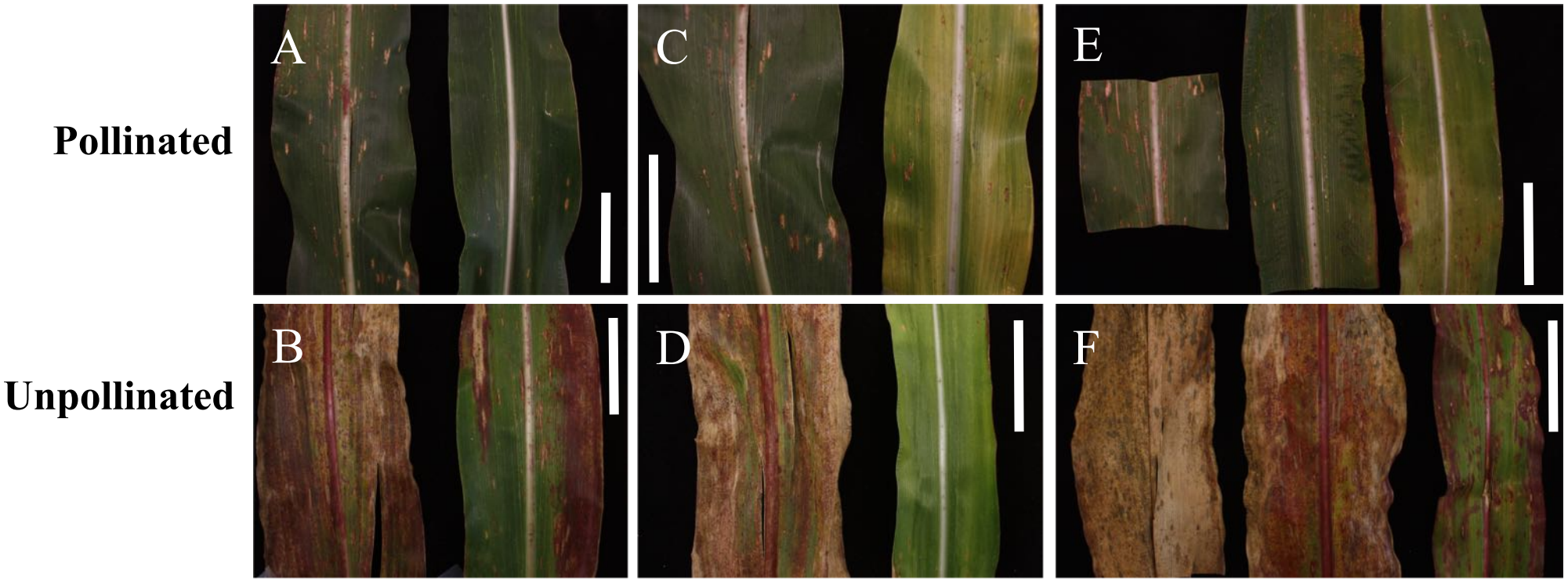

Figure 9. Effect of *vey1* on senescence induced by pollination prevention. Pictures of the representative primary ear leaf derived from plants at 30 and 40 days-after-anthesis (DAA) either with open pollinated (top panels: A, C, and E) or unpollinated (bottom panels: B, D, and F) ears. Representative primary ear leaf from (A-B) B73 wildtype (left) and mutant sibling (right) at 30DAA, (C-D) wildtype (left) and mutant (right) sibling from F_1 between B73-like NIL-b107 (with *vey1*^{Mo17} introgression) X *Oy1-N1989/oy1*:B73 at 30 DAA, (E-F) wildtype (B73-like NIL-b107), mutant B73-like NIL-b135 with *vey1*^{B73} (middle), and mutant B73-like NIL-b107 with *vey1*^{Mo17} (right) at 42 DAA. Scale bar in each figure is 6.35 cm.